Estimation of the effects of climate change scenarios on future Rhine water temperature development Extensive Version

IKSR
CIPR
ICBR

Internationale Kommission zum Schutz des Rheins

Commission Internationale pour la Protection du Rhin

Internationale Commissie ter Bescherming van de Rijn

Report No. 214

Modelling experts:
Ute Badde, Landesanstalt für Umwelt Baden-Württemberg (LUBW)
Dr. Tanja Bergfeld-Wiedemann, Bundesanstalt für Gewässerkunde (BfG)
Pascal Boderie, Institute for applied research on water, subsurface and infrastructure, The Netherlands. On behalf of Rijkswaterstaat, Water, Verkeer en Leefomgeving (WVL) (Deltares)
Dr. Gerhard Brahmer, Hessisches Landesamt für Umwelt und Geologie (HLUG)
Norbert Demuth, Landesanstalt für Umwelt, Wasserwirtschaft und Gewerbeaufsicht Rheinland-Pfalz (LUWG)
Ingo Haag-Wanka, Ingenieurgesellschaft für Umwelt und Wasserwirtschaft mbH, Karlsruhe (Hydron GmbH)
Sibylle Jacob, Landesamt für Natur, Umwelt und Verbraucherschutz Nordrhein-Westfalen (NRW)
Peter Krahe, Bundesanstalt für Gewässerkunde (BfG)

Imprint

Publisher:
International Commission for the Protection of the Rhine (ICPR)
Kaiserin-Augusta-Anlagen 15, D 56068 Koblenz
P.O. box 20 02 53, D 56002 Koblenz
Telefone +49-(0)261-94252-0, Fax +49-(0)261-94252-52
E-mail: sekretariat@iksr.de
www.iksr.org

ISBN-Nr 3-941994-53-0
© IKSR-CIPR-ICBR 2014

Estimation of the effects of climate change scenarios on future Rhine water temperature development

1. Summary

High water temperatures measured in the Middle and Lower Rhine, particularly in the summers of the years 2003 and 2006, led to a discussion of the topic "water temperature and climate change" at the conference of the ministers of the ICPR member states in charge of the protection of the Rhine in October 2007. In early 2013 the ICPR published reports on the development of Rhine water temperatures based on validated temperature measurements from 1978 to 2011 (ICPR 2013a) and on the current knowledge regarding the possible effects of changes in river discharge and water temperature on ecosystem behaviour and possible perspectives for action (ICPR 2013b). An expert group was created in July 2012 to prepare estimates of the future development of Rhine water temperatures from Basel to the Rhine Delta on the basis of assumed climate scenarios. This is their report.

The prognoses of future water temperatures are based on available hydrological models for the simulation of river discharge, in combination with water quality modules that simulate the associated water temperature. Available models were used, viz. LARSIM was applied for the river stretch from Basel to Köln, SOBEK for the stretch Worms to the Rhine Delta and QSim from Karlsruhe to Lobith. Validation of the models was performed using the hydro-meteorological measurements for the period 2001-2010 and actual heat discharges for selected periods within the reference period, for example the period July-September 2003.
The comparison of the validation results of the three models LARSIM, SOBEK and QSim shows good agreement between simulated and measured water temperatures, which certifies all models as valid for prognosis. Although the three models use different methods to simulate future water temperatures, this does not have any significant impact on the results.

The scenarios in this study relate to the scenario study of the ICPR (ICPR 2011) with the time horizons 2021–2050 (near future, NF) and 2071–2100 (far future, FF). The period 2001–2010 was set as the reference period for the evaluation of the future scenarios. The four future scenarios were composed by imposing two climate change scenarios for the near and far future on the actual meteorological data of the reference period in combination with two scenarios (Qmax and Qmin) for the low-flow river conditions (ICPR 2011). For all future scenarios 50% of the permitted heat discharges in 2010 were assumed. This percentage rate corresponds approximately to the mean actual heat discharges measured in the period 2001–2010.

In the near future,NF(2021–2050),the August water temperature in the Rhine shows an increase of about1ºC to 1.5ºC compared to the reference period (Ref50), while in the far future, FF(2071-2100), the increase in the average August water temperature is in the order of 3 to 3.5ºC. As expected the increase in water temperature is higher at lower flow rate (water temperature profile for Qmin is higher than Qmax). However, on average, the impact of the two different river discharge scenarios on water temperature is small compared to the change in water temperature resulting from (the meteorological effects of) the assumed climate change.

Natural variations in climate and river flow have led to significant variation in water temperatures over the years. The monthly averages for August 2003 are more than 3ºC warmer than the 10-year August average 2001–2010. Since the August 2003 values correspond roughly with the results of the future simulation, we can state that the extreme conditions experienced in August 2003 may serve as a model for the average summer situation in the far future (2071-2100).

Living organisms function only within a certain temperature range; outside this range, life activities such as reproduction are hampered. Water temperatures above 25°C cause stress in flora and fauna; for example, if fish are exposed for a longer period to water temperatures above 25°C their life expectancy decreases. In the near future, NF, the simulations show that the number of days with water temperatures above 25°C increase compared to the reference simulation run Ref50, while the number of days double at low river flow conditions (Qmin). In the far future, FF, the number of days exceeding 25°C will greatly increase. In Worms, for example, the numbers of days are simulated to increase from 11 to 74 compared to the reference run Ref50. This indicates that in the far future the water temperature at Worms in summer will, on average, be above 25°C for about 10 weeks. In the near future there will still be years where the critical value of 25°C will not be exceeded, in the far future this will be extremely rare.

2. Introduction

Historical high water temperatures in the Middle Rhine and German Lower Rhine during the summers of the years 2003 and 2006 renewed the attention for water temperature in relation to climate change. The ministers of the ICPR member states in charge of the protection of the Rhine summoned the ICPR to study the effects of climate change on the Rhine river basin, resulting in a literature overview of the state-of-the-art knowledge on the issue (ICPR 2009). In 2011 a study was published on the effects of climate change scenarios on the discharge regimes of the Rhine (ICPR 2011). The former study (ICPR 2009a) observed a knowledge gap with regard to the historical and future trends of water temperature in the Rhine. In early 2013 the ICPR (ICPR 2013a) published a report on long-term historical trends of water temperature.

Simulation models (LARSIM) were already implemented in upper parts of the Rhine basin for discharge prediction in the warm summer of 2003, and were then extended by means of a water temperature module. These models have since been successfully used for operational short-term forecasting and scenario simulations (e.g. Haag et al. 2005, Haag & Luce 2008, Kremer & Brahmer 2012).

The validated data 1978–2011 published in the report by the ICPR (ICPR 2013a) formed the basis for the models QSim and SOBEK, which were applied by BfG[1] and Deltares[2] in 2011–2012 for the simulation of the heat balance of the Rhine (Deltares 2012). One of the conclusions was that actual heat discharge data are required to properly validate such models.

To fulfil the ICPR assignment the following approach was accepted for the present study. The following existing models for the river Rhine will be involved: LARSIM applied by LUBW[3], LUWG[4] and HLUG[5], MIKE applied by LANUV[6] and QSim applied by BfG (all Germany) and SOBEK applied by RWS WVL [7](NL). The exact methodology is described in chapter 3. The following principles are used:

- Intrinsic properties of the individual models will not be altered, so as to do justice to different approaches towards understanding the behaviour of the river water system. Examples of such properties are the number of meteorological stations used

1 Bundesanstalt für Gewässerkunde
2 Institute for applied research on water, subsurface and infrastructure Netherlands. On behalf of Rijkswaterstaat Water, Verkeer en Leefomgeving (WVL).
3 Landesanstalt für Umwelt Baden-Württemberg
4 Landesamt für Umwelt Rheinland-Pfalz
5 Hessisches Landesamt für Umwelt und Geologie
6 Landesamt für Natur, Umwelt und Verbraucherschutz Nordrhein-Westfalen
7 RijkswaterstaatWater, Verkeer en Leefomgeving

as input, the interpolation methods and the simulation of the hydrology, the heat balance formulations etc.

- The data used by the different models are harmonised as far as practically possible. The models use the same validated data set as described and analysed by the ICPR (ICPR 2013a), e.g. the river discharge and water temperature measurements required at their upstream boundaries and measurements to demonstrate the validation of the models (chapter 3.2)
- Model performance is demonstrated (validation) using the actual heat discharge data of electrical power plants and industrial companies collected during this study
- To obtain uniform results, the future development of the water temperature of the Rhine (2021–2050 and 2071–2100) is based on two *connecting* models, viz. LARSIM (Basel up to Worms) and SOBEK (Worms up to Werkendam/Waal in the Rhine Delta)
- Additional information is presented based on simulations with three of the models (LARSIM, QSim and SOBEK) simulating water temperature for the Rhine stretch currently covered by these models (Fig. 3-2). Model results obtained for *overlapping* stretches of the Rhine will be used to quantify the variation of the model predictions.

Living organisms function only within a certain temperature range; outside this range activities such as reproduction are hampered. Temperatures above 25°C cause stress in flora and fauna; for example, if fish are exposed for a longer period to temperatures above 25°C their life expectancy decreases. Furthermore, temperature is an important parameter for all chemical and biological processes in surface water. For example, it dictates the rate of chemical processes, influences the amount of dissolved oxygen, and has an effect on the species composition of aquatic life. Direct and indirect effects of temperature affect the use of water, for example for the production of drinking water. A judgement on ecological aspects is beyond the scope of this study. Ecological aspects are described in ICPR 2013b. Results of this study may form the basis for a description of the consequences for the water quality, e.g. for the expert group on biological quality components.

The focus of this study is the effect of climate change on water temperature rather than on heat discharges. Future scenarios do not include the effects of potential changes in heat discharge which may result from socio-economic changes or other reasons in the future, such as energy policy. In other words, the effects of assumed climate change were studied by using the best estimate of current (2010) heat discharge inputs, knowing that these inputs have already changed in the last three years, for example, as Germany has been in the process of closing nuclear power plants since 2011.

3. Methods

River water temperature is a fundamental water quality parameter that exerts direct influence on river ecology, among other things. It is a limiting factor for the use of river water for industrial purposes. In particular, the input of cooling water from thermal power plants is commonly restricted by a water temperature threshold which may not be exceeded (LAWA 1991). The past and future changes in river water temperature may be caused not only by the direct influence of meteorological conditions, but also by changing river flows.

With respect to a rational long-term management of water resources it is of outstanding interest to have well-founded predictions of water temperature changes. Consequently,

the present study uses reliable deterministic simulation models to predict the combined effect of expected changes in meteorology and discharge on the future water temperature in the River Rhine.

This chapter describes the characteristics of the set-up of the model applications of the water temperature models, the validation of these model applications and the data used in the model applications for the predictions.

3.1 Description of the models

In this report a model is defined as an application of a more generic computer package or modelling tool. The three packages LARSIM, SOBEK, QSim have wider applications than the model applications for the Rhine presented in this report (Appendix B, C and D). Comprehensive descriptions of these computer packages are not part of this report.

All models simulate open channel river flow using numerical schemes. The flow modules of the models interface with the water quality solving the advection-diffusion equation numerically in 1-dimension (1D) based on a finite volume approach:

$$\frac{\partial T_W}{\partial t} + u \cdot \frac{\partial T_W}{\partial x} = D_x \cdot \frac{\partial^2 T_W}{\partial x^2} + S$$

where T_W = water temperature (°C), t = time (s), x = distance in flow direction, u = mean flow velocity (m/s), D_x = dispersion coefficient (m^2/s) and S = discharge of heat. The longitudinal river discharge (m^3/s) calculated by the 1Dflow module is used to calculate the mean velocity based on water level dependent cross sections in the models.

All models describe the heat exchange at the air-water interface following empirical relations for physical processes such as radiation, evaporation, conduction etc. Temperature changes caused by heat discharges (qds in energy per time unit) are taken explicitly into account. The heat exchange flux between water and the environment, such as the atmosphere and river bed, reads (W/m^2):

$$\mathbf{q_t = q_{sn} + q_{an} - q_{br} + q_L + q_{sg} + q_{rb} + q_{dis}}$$

with:

q_t	net radiation flux
q_{sn}	non-reflected (net) short wave radiation (sum of direct and diffuse) reaching the water
q_{an}	non-reflected (net) atmospheric radiation (long wave) entering the water
q_{br}	long wave back radiation from surface water
q_L	latent (non-sensible) heat flux by evaporation (-) or condensation (+)
q_{sg}	sensible heat of conduction
q_{rb}	heat exchange between water and (river) bed
q_{dis}	heat resulting from thermal discharges expressed per surface unit
q_a	long wave atmospheric radiation reaching the water surface (Figure 3-1)
q_{ar}	long wave atmospheric radiation reflected (Figure 3-1)
q_{sw},	short wave radiation (sum of direct and diffuse) reaching the water surface (Figure 3-1)
q_{sr}	short wave radiation reflected (Figure 3-1)

Changes in the water temperature (T_w) of a water layer (Δz) as a consequence of the total heat flux q_t ($W.m^{-2}$) can be calculated using the specific heat capacity definition:

$$\frac{\partial T_W}{\partial t} = \frac{q_t}{\rho_w . c_P . \Delta z}$$

Whereρ_w is the water density (kg.m^{-3}) and c_p the specific heat capacity (average value for water between 5 and 30°C equals 4 195 J.kg^{-1}.ºC $^{-1}$).

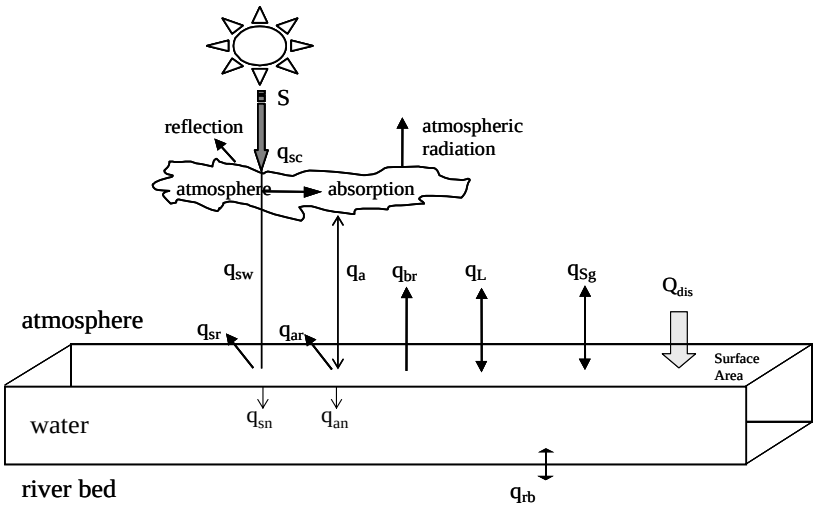

Figure 3-1: Heat fluxes across the air-water interface

In this chapter the three models used in this study, viz. LARSIM (3.1.1), SOBEK (3.1.2) and QSim (3.1.3) are described. The fourth model application which is used for the Rhine stretch from Bad Honnef to Lobith (Rhine-km 635-865) is MIKE 11. It is available at LANUV[8]. Due to time constraints the model is not used in this study and therefore not described here. Details on MIKE can be found at (http://mikebydhi.com/).

The area of the Rhine covered for the project is shown in Figure 3-2.

[8] Landesamt für Natur, Umwelt und Verbraucherschutz Nordrhein-Westfalen

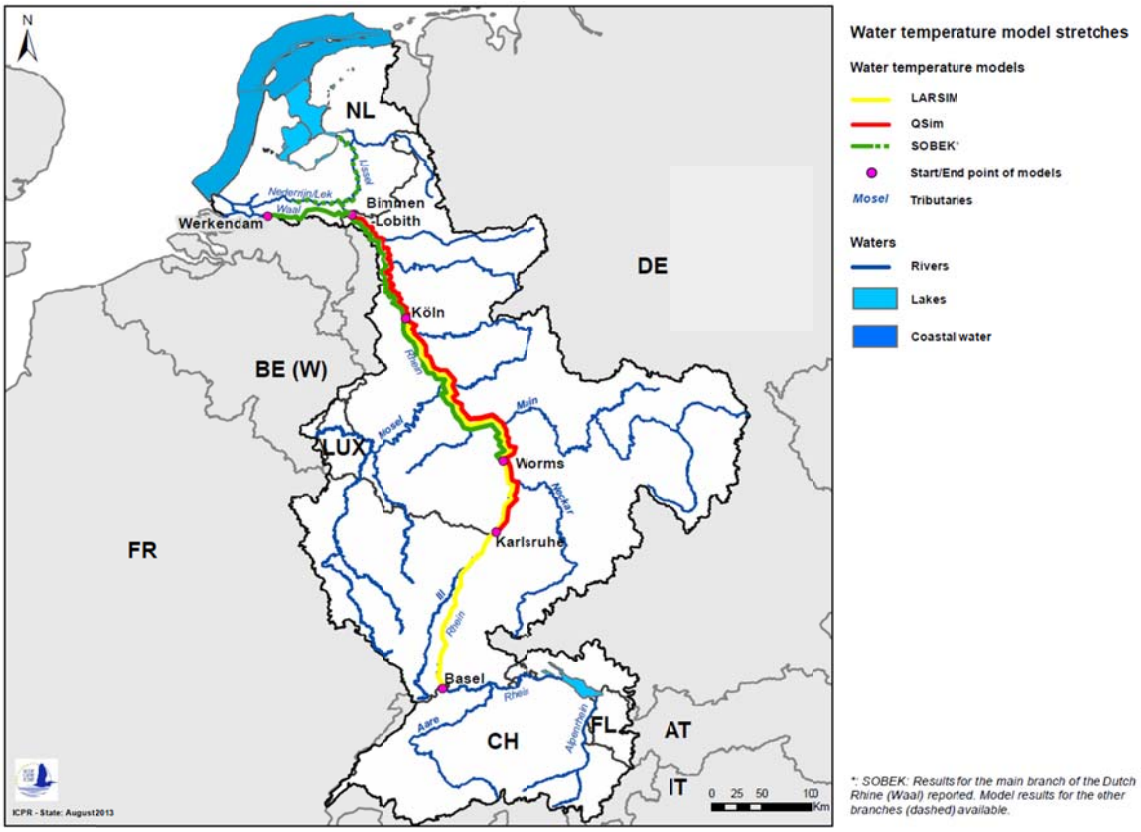

Figure 3-2: Map of the area covered by each of the three models LARSIM, QSim and SOBEK along the Rhine

3.1.1 LARSIM

The integrated water balance and water temperature model LARSIM-WWM is an extension of the water balance model LARSIM (Bremicker 2000). The addition of a water temperature module to LARSIM allows the simulation and forecast of discharges and river water temperatures across the entire river network of the modelled watershed (Haag et al. 2005, Haag & Luce 2008). LARSIM is driven by meteorological data for precipitation, air temperature, global radiation, humidity, wind speed, and air pressure. These forcing variables are internally interpolated from point measurements or numerical weather model grids to any simulation grid point within LARSIM. Within the physically-based water temperature module, heat transport in the river network is simulated with the one dimensional advection-dispersion equation (LfU 2005, Haag & Luce 2008).

In addition to this physically-based approach, LARSIM also allows the calculation of water temperature with regression models, which are valid for a specific location only. The non-linear regression models are based on the fundamental (logistic) interdependencies between air and water temperatures (e.g. Mohseni & Stefan 1999), the inertia of water with respect to heating, and the influence of river discharge on water temperature (for details see Haag & Luce 2008). These specific regression models are particularly well suited to define water temperature conditions at inflow boundaries of LARSIM and are used to calculate the water temperature of the model boundaries for the reference and the future scenarios. For more information see Appendix B.

Configuration of LARSIMfor the Rhine

There are two independent (but coupled) LARSIM models covering the 525 km stretch of the River Rhine from Basel up to Köln. The upstream model for the Upper River Rhine is operated by LUBW and covers the approx. 280 km long section between Basel and Worms. The downstream model for the Middle Rhine between Worms and Köln is run by HLUG and LUWG. At Worms, it is directly coupled with the upstream model (Kremer & Brahmer 2012, Figure 3-2).

The models include the Rhine along with its lateral canals and downstream sections of the rivers Main, Nahe, Lahn, Moselle and Sieg (Figure 3-3). Inflowing discharge and water temperature are considered for the upper boundary near Basel and a total of 39 tributaries. Discharge boundary conditions are either given by measurements or by simulation results of LARSIM. The present study does not make use of the existing LARSIM for the southern part of Hessen, the Neckar basin or the River Main. Rather, water temperature boundary conditions are calculated with specific regression models as described above at all boundaries.

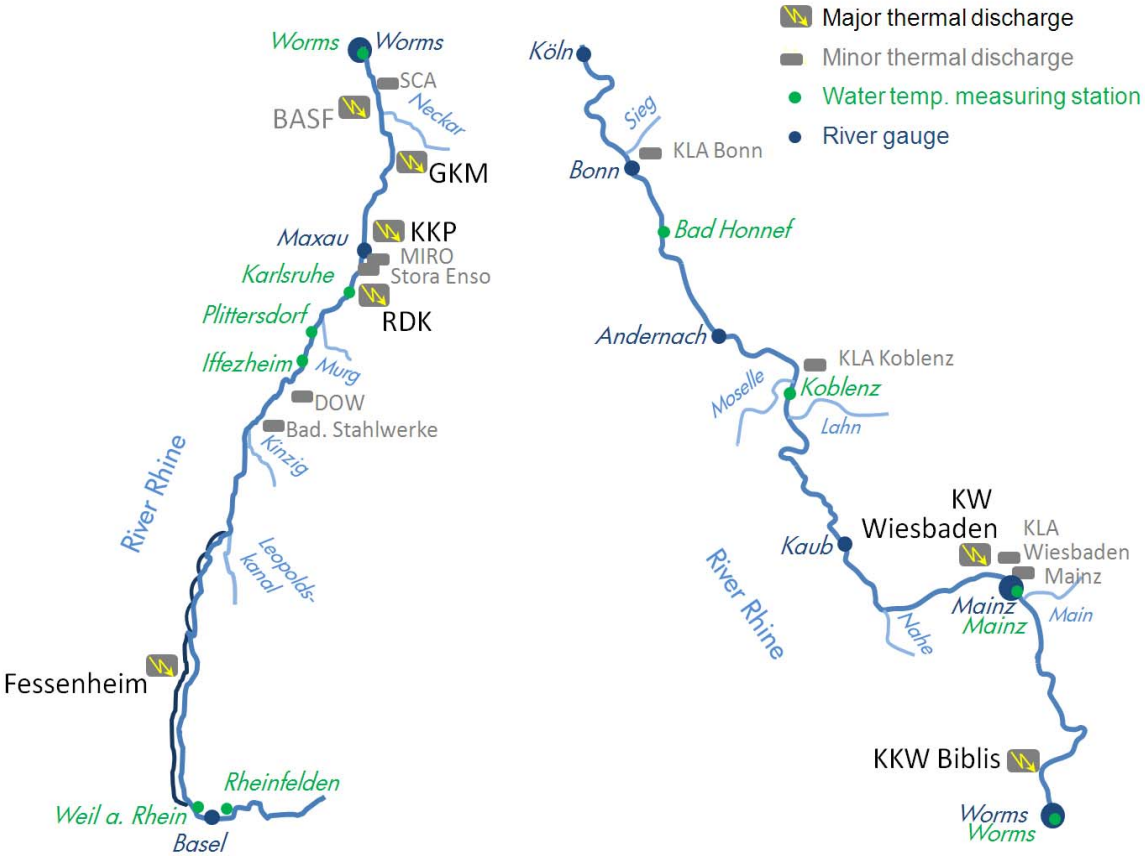

Figure 3-3: Schematic presentation of the Upper (left) and the Middle River Rhine (right) with gauging stations, water temperature measuring stations, and thermal discharge sites considered within LARSIM.

Discharge is routed through the system on the basis of volume-discharge-relations derived from the 1D hydrodynamic model. Transport behaviour, and thus also discharge routing, were checked and improved on the basis of the breakthrough curves of tracer experiments.

Water temperature within the model section is calculated with the physical model approach as described above. The models take the contribution of seven major thermal discharge sites into account. Minor thermal discharges from nine additional sources were taken into account for model calibration and validation, but neglected in model scenarios.

3.1.2 SOBEK

SOBEK is a modelling suite for the integral simulation of - among other things - flood forecasting, river morphology, and surface water quality, including water temperature. Two components of the system are used in this study viz. those for open channel hydraulics and water quality. The water quality module calculates the equilibrium temperature of the surface water as a result of atmospheric conditions (radiation, evaporation, conduction etc.). Temperature changes caused by heat discharge (energy per unit of time) are taken explicitly into account as well as the heat exchange between water and the environment, such as the atmosphere and the river bed. The third term in the energy budget of a river (Evans et al. 1998), being the heat flux due to friction, is ignored. For the physical background of the heat exchange at the air-water interface, Octavia et al. (1977), Sweers (1976), Gill (1982) and Lane (1989) are suitable references. For more information see Appendix C.

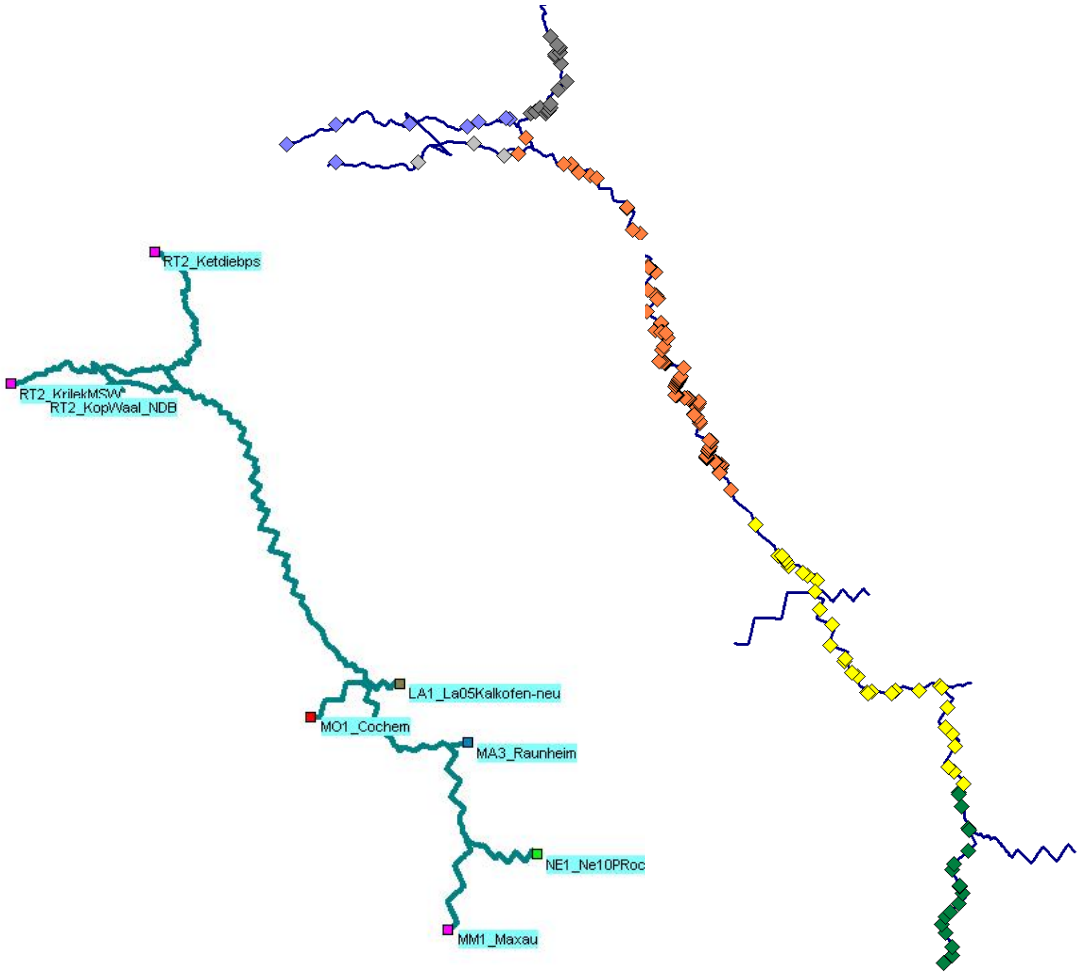

Figure 3-4: SOBEK schematisation of the Rhine model boundaries (left) and several other tributaries and lateral inflows (HBV simulated) clustered in four regions (right, symbols).

Configuration of SOBEK for the Rhine
The SOBEKmodel covers the Rhine stretch from Maxau (Rhine-km 362) to Werkendam (Rhine-km 967 - Waal) in the Netherlands Delta of the Rhine branch Waal. Model output is generated at the nearby water quality measurement station at Woudrichem (Rhine-km958 - Waal). SOBEK upstream boundaries are located at Maxau, Neckar at Rockenau, Main at Raunheim, Lahn at Kalkofen and Moselle at Cochem (Figure 3-4).

Discharge and water temperature are required for all boundaries and tributaries. Discharges at the boundaries and tributaries are either measured or simulated by the rainfall runoff model HBV (BfG 2005); the former prevails when available. Water temperature at the boundaries is either measured or calculated using simple linear regression formulae based on a 9-day running average of the air temperature; the former prevails when available. Four different linear regressions are used to cover the smaller tributaries and laterals according to the clustering shown in Figure 3-4, using air temperature from the closest meteorological station.

Within the model schematization, discharge and water temperature are calculated using the 1D hydrodynamic model (flow) coupled with the physically-based water quality module (WAQ).
Discharge and water temperature at the model boundaries were provided by the German State authorities or the BfG (ICPR 2013a). SOBEK uses the same daily meteorological data as QSim, data were provided by DWD for stations at Karlsruhe/Rheinstetten, Frankfurt airport and Düsseldorf. Global radiation data are calculated from sunshine duration measured at Mannheim, Geisenheim and Bochum respectively (Prescott 1940). For the Netherlands section of the Rhine, the de Bilt station is used, for which KNMI provided the measurements.

3.1.3 QSim

The water quality model QSim describes in a mathematical way the predominant complex chemical and biological processes in running waters (Kirchesch & Schöl 1999). QSim was established in 1980 and has been expanded and improved constantly since at the German Federal Institute of Hydrology (BfG). QSim is a deterministic model, meaning that the processes relevant for the temperature regime of a river are described functionally in the form of differential and algebraic equations without any stochastic effect. The identification and parameterisation of the mathematical functions are based on published scientific knowledge or on our own experimental results. If this is not sufficient, empirical equations are used. The variables are considered to be homogeneously distributed across the river's cross section (one-dimensional model). QSim is connected with the standalone one-dimensional hydrodynamic model HYDRAX, which calculates discharge, water level and flow velocity in running waters (Oppermann 1989 and 2010). The discharge can be calculated either in a stationary (no change of discharge during the model run) or dynamic non-stationary way (changing discharge during the model run). HYDRAX and QSim are combined with each other by the graphical user interface GERRIS.
The driving forces of the water temperature module are the discharge at the upper boundary (the starting point of the model section) and of the main tributaries, as well as meteorological conditions (global radiation, air temperature, evaporation, cloudiness, wind velocity). All variables in QSim depending on solar radiation (including the temperature module) are modelled dynamically at an interval of one hour. The module used to simulate the water temperature in QSim is described in detail in Appendix D.
Recent publications are Becker et al. (2009) and Quiel et al. (2011). For more information see http://www.bafg.de/DE/08_Ref/U2/01_mikrobiologie/QSIM/qsim.html and Appendix D.

Configuration of QSim for the Rhine

The QSim model covers the Rhine stretch from Karlsruhe (Rhine–km359) to Lobith (Rhine-km865) (Figure 3-5). The morphological conditions of this 500 km Rhine stretch are derived from gauged cross sections every 500 m from 2004 (digital terrain model (DGM) WSD West P-2004.prf). This information was used by the BfG to build the Rhine model (Hardenbicker 2013). The 11 major tributaries and 16 heat discharge sites shown in Figure 3-5 are taken into account. In QSim, three weather stations are implemented (data from DWD,Figure 3-5). Global radiation is not measured at every weather station; as a consequence different nearby stations had to be used for this parameter.

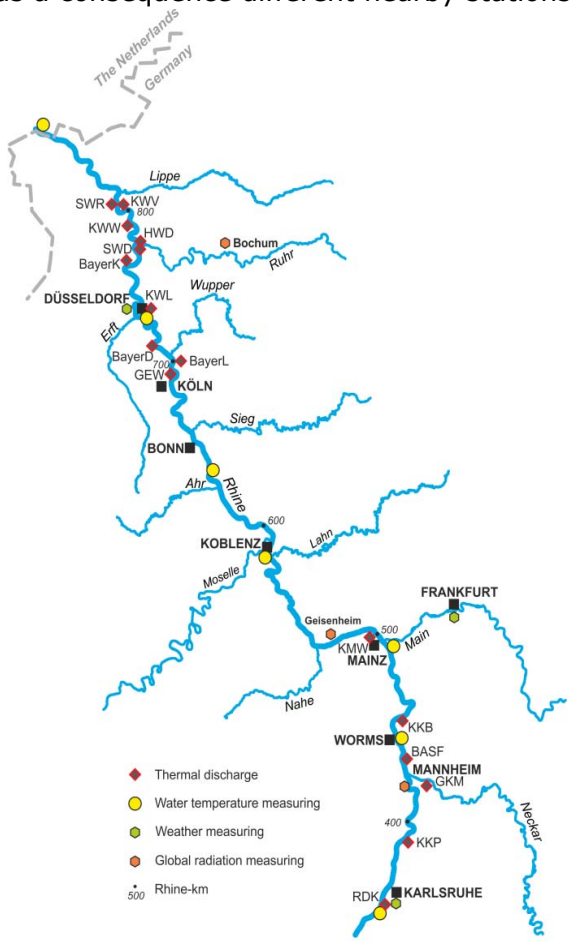

Figure 3-5: QSim schematisation of the Rhine from Karlsruhe (Rhine-km 359) to Lobith (Rhine-km 865). The implemented heat discharge sites, tributaries, water temperature, weather and global radiation measuring stations are shown.

Discharge and water temperature at the model boundaries were provided by the German State authorities or the BfG itself (ICPR 2013a). Missing water temperature measurements were simulated with QSim with the aid of a local surface water body (LSWB) model. For the weather stations, the resulting water temperature in the LSWB was simulated. The upper model boundary at Karlsruhe and the tributaries were allocated to the closest weather station according to their position (Table 3-1) and the relation between the measured water temperature and that simulated with the LSWB was used to calculate the missing data.

Table 3-1: Weather and global radiation stations used in QSim(data from DWD) and attributed Rhine stretches.

Rhine-km		Weather data	Global radiation
From	to	Station	Station
359.0	469.5	Karlsruhe/Rheinstetten	Mannheim
469.5	601.5	Frankfurt Airport	Geisenheim
601.5	865.5	Düsseldorf	Bochum

For this report, the QSim version 13.0 (from 12/06/2012), the HYDRAX-version 4.2 from 08/10/2010 and the GERRIS version 1.6.8 were used.

3.2 Model Validation

The models used in this study have been developed, calibrated and applied prior to this study. In this study the existing models were used as much as possible as they are available. Calibration of the models is therefore not part of the study. In this chapter the models were validated by comparing the simulation results with measurements of the Rhine water temperature. A good agreement between model results and measurements provides confidence in the models and thus in the predictions of the future water temperatures made by these models.

The models described in chapter 3.1 are applied to predict water temperature for the period 2001-2010. This period was selected as validated water temperature data were available for this period (ICPR 2013a). Furthermore the period is long enough to show natural annual variations, as it contains, for example, two extremely warm years (2003, 2006) and a cold year (2009). The models are driven by time series of meteorology, discharge and water temperatures at their boundaries.

In the validation runs, LARSIM used the actual (major) heat input data 2001-2010 on a daily basis. QSim and SOBEK could select 7 months of this 10-yearperiod for validation, where the actual heat input of power plants greater than 200 MW was provided. The provision of the heat input is an important improvement compared to the use of permitted discharges, which was the previous working procedure (Deltares 2011). The following periods were chosen:

- July-September 2003
- November-December 2005
- April 2007
- September 2008.

3.2.1 Actual heat discharges

In this study detailed information on actual heat discharges, mostly daily values, in Germany and the Netherlands were collected and used in the model validation. The purpose of this analysis is to access how the actual heat discharges relate to the permitted discharges and how the ratio between the actual and permitted discharge varies among the industries and over the seasons.

In total, data were obtained for 15 dischargers upstream of Lobith with a total of 14,390 MW permitted discharges and 13 downstream of Lobith with a total of 10,857 MW permitted discharges.

The following observations are relevant:

- The yearly averaged actual heat input equals 50% of the permitted heat discharge for the German and 46% for the Dutch part.
- The actual heat input in August 2003 is 34% of the permitted discharge, this value is reliable as data from all actual heat inputs were available for this month.
- Variation of the ratio actual/permitted for other months is less reliable as the data set on heat inputs is not complete. As an indication, the ratio varies from 69% in January to 40% in November and 45% in July-August (Germany). The ratio is fairly constant for the Dutch part of the plants (43 to 48%).
- Obviously the percentages for the individual heat discharges vary considerably.

The above implies that a fixed ratio of actual/permitted heat discharge of 50% will be used for the reference situation for the climate scenarios (see 3.3). It also means that the reference run (Ref50 using 50% of the permitted heat discharges) and the validation (using actual heat discharges) are not the same.

3.2.2 Results of the model validation

Model results of discharge and water temperature were evaluated for LARSIM, QSim and SOBEK (not presented in this study). To summarise the model validations, the relation between measured and modelled water temperature is shown at Koblenz for each model (Figure 3-7). In addition, two coefficients indicating model efficiency (Nash-Sutcliffe, nse[9] and the root-mean-square error, rmse[10]) were calculated for several locations covered by each model (Table 3-2).
The number of measurements varies for the locations. The number of observations used to determine the coefficients (n) also varies, as the models are run for varying periods: LARSIM (Basel-Worms) uses 5 years of data, LARSIM (Worms-Köln) 10 years of data and SOBEK and QSim are compared with measurements for 7 months.

Table 3-2: The Nash-Sutcliffe model efficiency coefficient (nse, dimensionless) and the root-mean-square error (rmse, °C) based on daily water temperature values.

	RhineKm	335	340	359	443	498	591	640	730	862
	Location	**Iffezheim**	**Plittersdorf**	**Karlsruhe**	**Worms**	**Mainz**	**Koblenz**	**Bad Honnef**	**Düsseldorf**	**Lobith**
LARSIM	nse (-)	0.996	0.996	0.996	0.997	0.999	0.998	0.999		
validation 2001–2010	rmse (°C)	0.37	0.37	0.37	0.37	0.26	0.31	0.32		
	n	1 700	1 822	1 771	1 771	3 256	3 619	2 651		
QSim	nse (-)				0.964	0.985	0.977	0.978	0.937	0.952
validation period	rmse (°C)				0.52	0.48	0.47	0.51	0.57	0.52
	n				213	213	213	177	137	187
SOBEK	nse (-)				0.96	0.977	0.980	0.987	0.973	0.984
validation period	rmse (°C)				1.32	1.02	0.89	0.75	0.89	0.86
	n				213	213	213	177	138	187

[9] Dimensionless coefficient defined as 1- data variance / residual variance. nse = 1 indicates a perfect match between model and observations, nse = 0 indicates that the model predictions are as accurate as the mean of the observed data.

[10] rmse is defined as the root of the mean square of the residues, same unit as the data (°C T in this case)

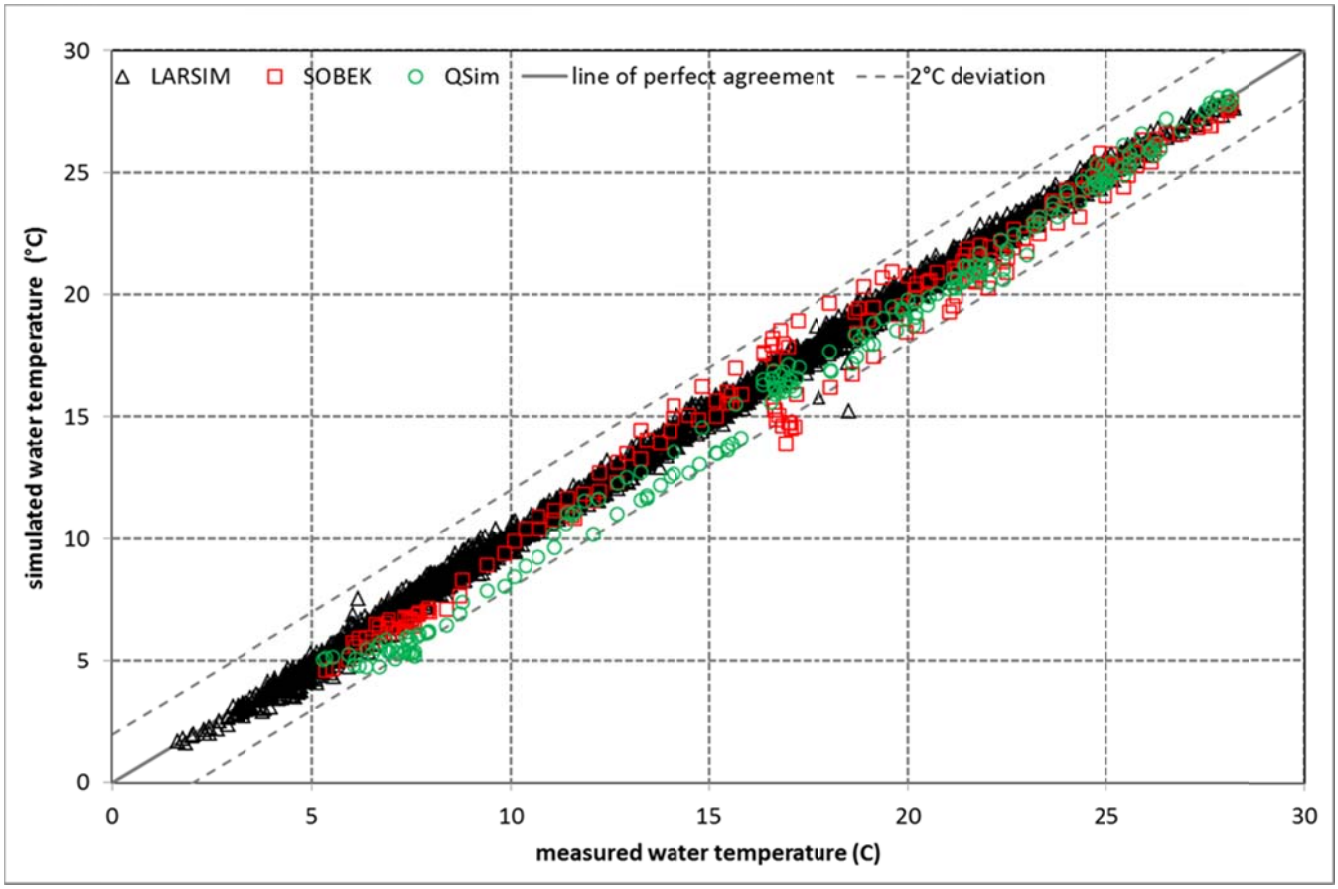

Figure 3-6: Scatter plot of simulated (vertical) and measured (horizontal) water temperature at Koblenz (Rhine-km 590) for the three models. The dashed lines indicate a 2ºC deviation from the ideal 1:1 ratio (solid line).

3.2.3. Conclusions model validation

The overall performance of the models is determined by both the physical part (inside the schematised model area) and by the regression part. The performance presented in this chapter is the overall performance.

All three models show (more than) adequate resemblance with the observations and can be used for reliable future predictions of the water temperature under different climate and heat discharge scenarios.

Essentially, the closer the model efficiency (nse) is to 1, the more accurate the model is. LARSIM has the best fit to the measurement data, while QSim and SOBEK show comparable accuracy. This is explained by the more advanced regression model and the much larger amount of meteorological input data in LARSIM. This study did not compare the performance of the physical models separately.

From the scatter plots, QSim shows notable underestimation of the lower water temperatures. SOBEK shows no bias but less precision (higher spread).

3.3 Data used in the scenarios

Future scenarios are simulated by the models through a 10-year simulation run similar to the validation period 2001 to 2010. There are two scenario runs representing the near

(2021–2050) and the far (2071-2100) future and one reference run to compare against. An additional simulation of the reference condition is made without heat inputs to assess the anthropogenic influence.

For the reference and scenario runs the following model inputs are altered compared to the validation runs:

- heat inputs (3.3.1)
- meteorology, atmospheric conditions (3.3.2)
- river discharge (3.3.3)

The future model forcing is described in this chapter and summarized below in Table 3-3.

The reference run (Ref50) uses a representation of the current situation using the same measurements for meteorology and discharge as used for the validation runs. The heat discharges in the reference run (Ref50) and all future scenarios are set at 50% of the permitted direct heat inputs in 2010 (see 3.3).

The additional natural situation run (Ref0) uses no heat inputs at all. This run is made to assess the impact of heat discharges on water temperature in the reference situation.

For the future scenario runs the meteorological measurements (2001–2010) are modified using assumed climate change vectors described by BfG (BfG 2013). For the future river discharges the historical measurements (2001–2010) at the model boundaries are modified using prognoses of NMQ7 values, differentiated for the hydrological summer and winter (ICPR 2011). The heat discharges in the future are assumed to be the same as those in the reference situation (Ref50).
In section 3.3.4 it is explained how the water temperatures at the boundaries of the models are derived from changes in meteorology and discharges as described in Table 3-3.

Table 3-3: Definition of the model forcing used in the scenario runs

No.	Name	Model simulations	Period	Heat discharge	Atmosphere	Summer discharge	Winter discharge
1	Reference (Ref50)	Reference (current) with heat inputs	2001-2010	50% of permitted 2010	2001-2010	2001-2010	2001-2010
2	Ref. no heat input (Ref0)	Reference (current) without heat inputs	2001-2010	no heat input	2001-2010	2001-2010	2001-2010
3	NF+Qmax	Scenario for the near future with maximum river discharge and heat inputs as in Ref50	2021-2050	50% of permitted 2010	Average summer air temperature +1.5°C	+10%	+15%
4	NF+Qmin	Scenario for the near future with minimum river discharge and heat inputs as in Ref50	2021-2050	50% of permitted 2010	Average summer air temperature +1.5°C	10%	0%
5	FF+Qmax	Scenario for the far future with maximum river discharge and heat inputs as in Ref50	2071-2100	50% of permitted 2010	Average summer air temperature +4°C	10%	+15%
6	FF+Qmin	Scenario for the far future with minimum river discharge and heat inputs as in Ref50	2071-2100	50% of permitted 2010	Average summer air temperature +4°C	25%	5%

3.3.1 Future heat discharges

The real daily heat discharges collected 2001–2010 cannot be used for the scenarios as they vary greatly depending on maintenance, prevailing water temperature of the Rhine etc. As described in chapter 3.2.1, it was decided to use 50% of the permitted heat discharge for the reference scenario and the future scenarios. Although the data in the inventory gave some indication that this percentage is typically somewhat higher in winter and lower in summer, the decision was taken not to differentiate the percentage over time. Only direct heat inputs with permitted values of more than 200 MW were taken into consideration (Table 3-4). These simplifications seem to be reasonable, because the main focus of this work is the prediction of the effect of climate change on water temperature and not the influence of heat discharges.

Table 3-4: Permitted heat inputs from 2010 and values used for the scenario simulations (direct heat inputs with permitted value >200 MW).

	Rhine-km	Permitted heat input (MW)	Scenarios used (MW)
KKW Fessenheim	212.4	3 600	1 800
Rhein-Dampfkraftwerk Karlsruhe	359.5	1 175	587.5
KKW Philippsburg	389.5	4 265	2 132.5
Großkraftwerk Mannheim (June-Sep.)	416.5	1 014	507.0
Großkraftwerk Mannheim (Oct.-May)	416.5	2 027	1013.5
BASF Ludwigshafen, Kühlwasser	433.0	2 257	1128.5
KKW Biblis*	455.0	1 674*	1 674*
Kraftwerke Mainz-Wiesbaden	502.0	785	392.5
GEW Köln AG, Köln	694.0	394	197
Bayer AG, Leverkusen	700.0	611	305.5
Bayer AG/EC Dormagen	710.0	268	134
KW Lausward, Düsseldorf	740.5	770	385
Bayer AG, KR Uerdingen	766.0	461	230.5
KW SW Duisburg	777.0	720	360
KW Herm. Wenzel, Duisburg	781.0	545	272.5
STEAG Walsum	792.0	710	355
STEAG Voerde	799.0	820	410
Solvay, Rheinberg	808.0	208	104
Electrabel Nijmegen (Waal)	886.0	790	395
ElectrabelHarculo (IJssel)	-	670	335

* Permitted discharge at low river discharge

3.3.2 Future climate

It was decided to select two climate scenarios viz. ”increased summer temperature + 1.5 K” and ”increased summer temperature + 4 K” as representative projections for the near (2021–2050) and far (2071–2100) future. Assumed climate change vectors are based on the EU project ENSEMBLES. The climate-model-chains Arpege-Aladin51 (2021/50-1971/00) and HadleyQ0-CLM (2071/00-1971/00) are used to quantify monthly varying assumed climate change vectors for air temperature, humidity, global radiation, air pressure, wind velocity, cloud cover and precipitation on a 50 x 50 km raster covering the Rhine basin.

Details on the assumed climate change vectors, the motivation of the choice of the climate models used for the prediction, and the details of the data handling procedures to arrive at the vectors are reported by BfG (2013).

For each of the two atmospheric scenarios the assumed climate change vectors are available for:

- six relevant meteorological variables, viz. air temperature (mean, minimum and maximum value), relative humidity, global radiation, air pressure, wind velocity, cloud cover and precipitation
- each month of the year
- 20 grids (50 x 50 km) along the rivers Moselle, Main and Rhine running from Basel to the North Sea

It was decided to work as much as possible with the existing models LARSIM, QSim and SOBEK, although this approach implicates differences in the model results. For example, in 2010 SOBEK used data from 10 DWD stations. In 2011, to harmonise the QSim and SOBEK results for a combined project (Deltares 2011), three meteorological stations characteristic for the south, middle and northern part of the German part of the Rhine catchment were used by SOBEK.
In order to run SOBEK and QSim for the climate scenarios, the meteorological forcing (time series) of the three meteorological stations in use is altered using the assumed climate change vectors given by BfG (2013).Table 3-5 summarises the raster used to alter the three meteorological stations for the two climate scenarios. In contrast LARSIM uses the spatially distributed information of all 50x50 km grids along the modelled river stretch.

Table 3-5: Link between meteorological stations (used in QSim and SOBEK) and the Raster ID for which climate change vectors are calculated.

	Meteorological Station used in QSim and SOBEK	**Raster**	
Station 1	Düsseldorf	15	North
Station 2	Frankfurt	11	Middle
Station 3	Karlsruhe	9	South
Station 4	De Bilt	19	Netherlands

As assumed climate change is expected to have its largest impact through changes in meteorology and not in future discharge, the assumed climate change vectors are shown here graphically (Figure 3-7) (for data see Appendix A).

Figure 3-7 shows:

- Regional differences are generally not very pronounced (maximum 0.4°C in air temperature in the far future).
- Maximum air temperature increase in August, in the near future +2°C and in the far future +4.5°C.
- A pronounced increase in global radiation in the far future, notably in September.
- Relative humidity decreases significantly in summer months (5% in the near and 10% in the far future) with the exception of the North, where the reduction is less pronounced in the far future.
- Cloudiness increases in the far future and
- there is less wind in the far future around September.

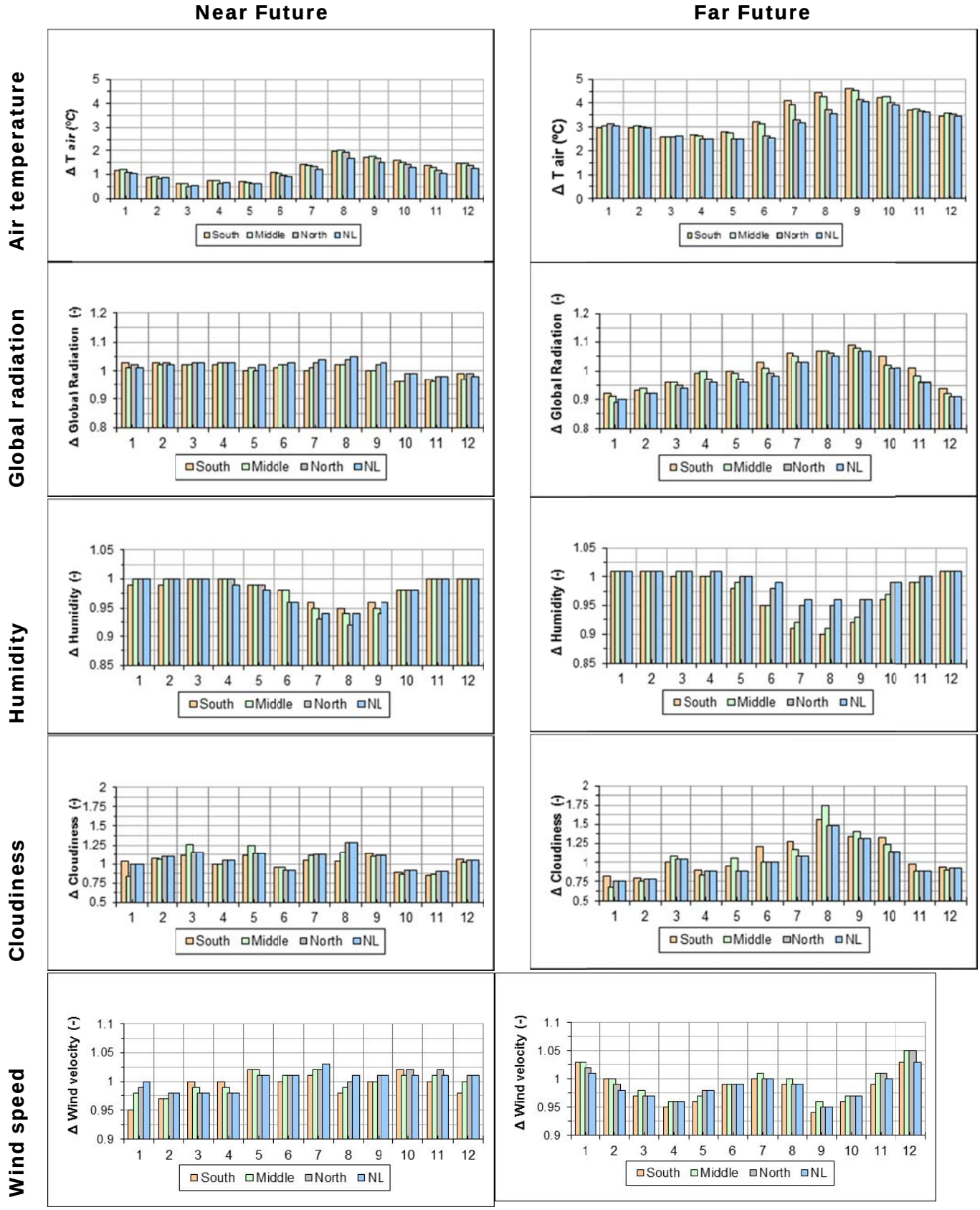

Figure 3-7: Monthly assumed climate change vectors for five meteorological variables (air temperature, global radiation, humidity, cloudiness and wind velocity) for the near (left column) and far (right column) future for three representative locations in south, middle and north Germany and the Netherlands.

3.3.3 Future river discharges

The future discharges feeding the water temperature models in this study follow ICPR 2011 and are based on a relative change in low-flow conditions for the future. The relative changes are summarized in Table 3.3 and are based on a river basin approach followed in ICPR 2011 (ICPR, Report 188, Table 4). The relative changes in river discharges are defined for two future periods, viz. the near (2021–2050) and far (2071–2010) future and are relative to the period 1961-1990.

The relative changes in river discharge distinguish between the hydrological summer (April/May to October) and the hydrological winter (November to April) because this study focuses both on potential future problems with summer water temperatures as well as on future winter temperatures (below 3 ºC).

3.3.4 Future water temperatures at model boundaries

In this section it is illustrated how the models translate the climate change vectors to water temperature at their (upper) model boundaries and tributaries.

LARSIM uses its nonlinear regression model to calculate water temperature at the boundaries in response to air temperature and discharge. For the purpose of future water temperature the regression model is fed with a prognosis of river discharge and meteorological conditions. The assumption is that the current correlation between water temperature and river discharge and air temperature is still valid in the future climate. This may not be a realistic assumption, especially in the far future when the assumed climate change vectors cause air temperature to be outside the range for which the regression model is made.

QSim and SOBEK take a delta change (+ ΔT) approach for their boundary water temperature values in the future scenario runs. The delta change is based on the response of a local surface water model to the full set of meteorological climate change vectors. The local surface water temperature model (a simplified 4 m deep water body) is run twice, once using the current (2001–2010) meteorological conditions and once with the future meteorological conditions. The difference in simulated water temperature (ΔT) is added to the (measured) water temperatures of the reference run to obtain the water temperature conditions at the model boundaries for the scenario runs. The reason for following this approach is that it includes feedback mechanisms, such as evaporation, which determine the response of surface water temperature to imposed climate change vectors including air temperature, radiation, cloudiness, wind, etc.
Figure 3-8 shows the change in water temperature (ΔT) in the far future scenario at the water mouth of the Main. All three models cover the water mouth of the Main with their simulations (Figure 3-2). Being the main driving force for water temperature, Figure 3-8 also shows the assumed climate vector for air temperature against the time of the year. From Figure 3-8 the following observations are made:

- Higher discharge (Qmax compared to Qmin) leads to lower water temperature (effect approximately 0.4°C) for LARSIM.
- The water temperature follows the air temperature with a delay of approximately one month
- For the far future (FF+Qmin) the summer air temperature vector (+ 4.6°C) causes the strongest change in water temperature for LARSIM (+4.7°C in September), whereas the response of QSim and SOBEK is more subdued (+4.3°C and 4.2°C in September respectively)

- In winter (FF+Qmin) the increase in the February air temperature (+3°C) results in a water temperature rise in February of +2.5°C in LARSIM, +1.8°C in QSim and 2.1°C in SOBEK

It is relevant to realise that although the input of the models is harmonised with respect to the assumed climate change effects on meteorology and river discharge, the models use fundamentally different approaches to translate the assumed climate change vectors into water temperature at their model boundaries. As LARSIM does not take account of feedback mechanisms at higher water temperatures, it probably overestimates the far future water temperature at the boundaries. The difference between LARSIM on the one hand and QSim and SOBEK on the other hand is 0.5 ºC in the far future.

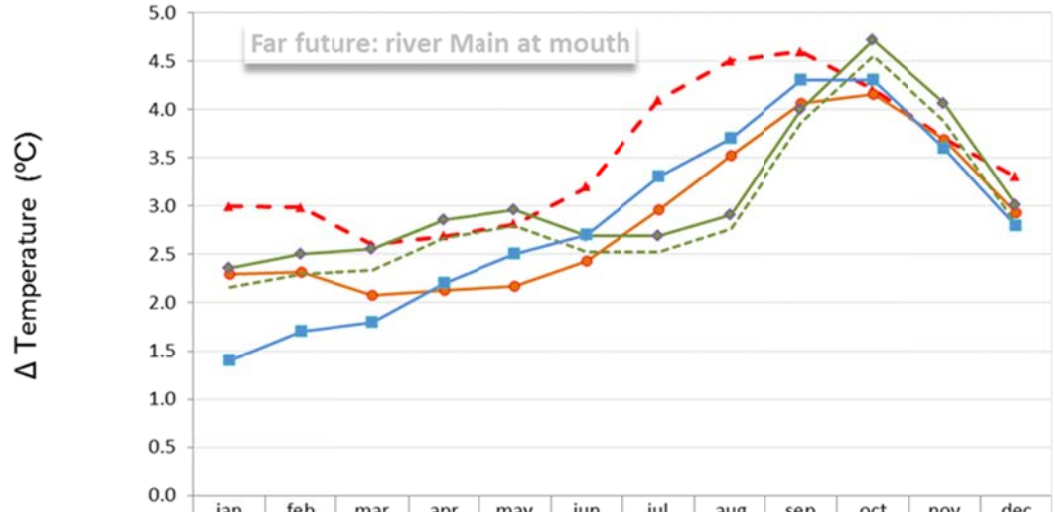

	jan	feb	mar	apr	may	jun	jul	aug	sep	oct	nov	dec
Air	3.0	3.0	2.6	2.7	2.8	3.2	4.1	4.5	4.6	4.2	3.7	3.3
SOBEK	2.3	2.3	2.1	2.1	2.2	2.4	3.0	3.5	4.1	4.2	3.7	2.9
LARSIM FF-Qmax	2.2	2.3	2.3	2.7	2.8	2.5	2.5	2.8	3.9	4.6	3.9	2.8
LARSIM FF-Qmin	2.4	2.5	2.6	2.9	3.0	2.7	2.7	2.9	4.0	4.7	4.1	3.0
QSim	1.4	1.7	1.8	2.2	2.5	2.7	3.3	3.7	4.3	4.3	3.6	2.8

Figure 3-8: Monthly averaged air temperature vector (ΔT, °C) for the assumed climate change in the far future (dashed line) and resulting water temperature vector (ΔT, °C) at the model boundaries at the water mouth of the Main as applied in LARSIM, QSim and SOBEK. Water temperature vector based on (1) non-linear regression of water temperature with river discharge and air temperature for LARSIM or (2) response of a local surface water body of 4m depth using full climate vectors for QSim and SOBEK.

4. Results and Discussion

The development of the water temperature of the Rhine in the near (2021–2050) and far (2071–2100) future is presented in chapter 4.1. The results in 4.1 are based on two connecting models, viz. LARSIM (Basel up to Worms) and SOBEK (Worms up to the mouth of the Rhine Delta in the Netherlands).

Additional results based on simulations with the three models that were applied in this study (LARSIM, QSim and SOBEK) are presented in chapter 4.2. Multiple predictions for overlapping stretches of the river Rhine reveal the variation caused by the application of different models.

4.1 Results for Basel – Delta

In this paragraph the results for the Rhine running from Basel to the River Delta in the Netherlands are presented. The results are based on simulations by LARSIM for the stretch Basel to Worms followed by simulations with SOBEK from Worms to the Rhine Delta in the Netherlands. At the transfer point in Worms, SOBEK starts using the water temperature simulated by LARSIM for all simulations.

4.1.1 Temperature profile of the Rhine

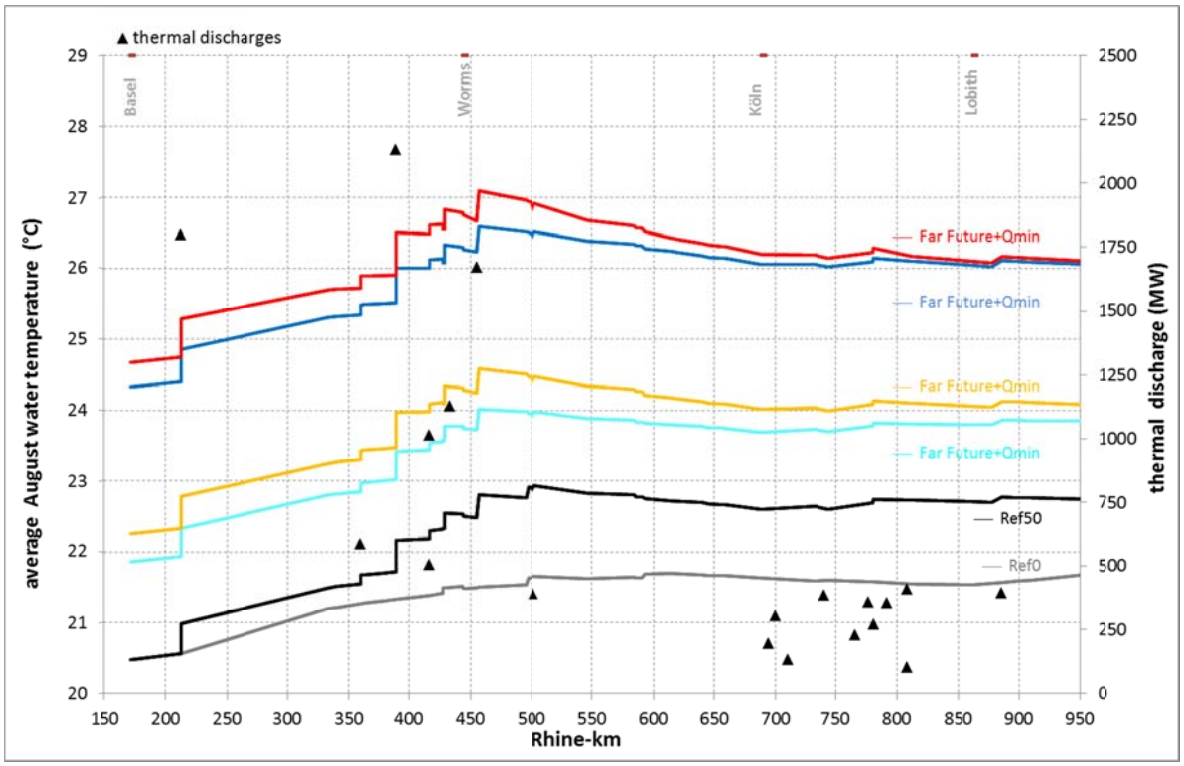

Figure 4-1: Longitudinal profile in the Rhine (Basel-Delta) of average August water temperature (°C) simulated by LARSIM (Basel – Worms) and SOBEK (Worms-Werkendam)

Figure 4-1 shows the development of the average August water temperature in the Rhine. For Ref50 relatively cold water of 20.5°C at Basel heats up to nearly 23°C at Mainz (Rhine-km500). Further downstream the water cools down, reaching 22.6°C at Düsseldorf (Rhine-km700), thereafter the average August temperature builds up slightly again to 23.8°C around the German-Dutch border (Rhine-km850). The profile of the natural water temperature without heat input (Ref0) also shows the gradual warming of the Rhine water; the strongest warming takes place in the Upper Rhine up to Worms.

The "peaks" in the longitudinal water temperature profile in the reference run are the result of thermal inputs to the river, as can be seen when comparing the longitudinal plots for the reference run with and without thermal discharges (Ref50 vs. Ref0): the stepwise increase of water temperature coincides with the location of the thermal discharges (black symbols in Figure 4-1). During average summer conditions in the reference scenario (Ref50), the thermal heat inputs cause the water temperature to increase by 1 to 1.5°C.

While interpreting Figure 4-1 one should bear in mind that (1) the water temperatures are monthly average values for August for a 10-yearperiod with varying hydrological and meteorological conditions and (2) river discharge in summer generally increases towards the delta, resulting in a larger dilution. Thus, further upstream a thermal discharge leads to a larger increase in water temperature than would be the case if the same amount of heat were disposed further downstream, where river discharge and dilution are greater.

In addition, Figure 4-1 shows the impact of the assumed climate change on water temperature for the near and far future at high and low river discharge scenarios. At first glance the longitudinal profiles for water temperature look similar to those for the reference situation with the proviso that assumed climate change causes water temperatures to be 1-1.5°C higher in the near and 3-4°C higher in the far future, resulting graphically in a vertical shift of the profiles.

As expected, the increase in water temperature is less with higher river discharge (Qmax) and higher with lower river discharge (Qmin). The temperature effect of variation in river discharge is relatively small (the range in water temperature caused by variation in river discharge is 0.2-0.5°C at maximum) compared to the impact caused by the atmospheric heat balance effect of assumed climate change.

At the upper model boundary at Basel, LARSIM uses elevated water temperatures for the low discharge situation (average August water temperature for Qmin is approximately 0.4°C higher than for Qmax, see chapter 3.3). Additionally, low river discharges lead to higher water temperatures as thermal discharges are diluted less by lower river discharges. Figure 4-1 shows that the difference between the simulated water temperature for Qmax and Qmin thus dissipates further downstream and that this effect seems to be more or less the same for the near and the far future (which seems logical, as the reduction of river discharge for the far and near future summers are almost equal) (NF: Qmin/Qmax = (100%-10%)/(100%+10%) = 81% and FF: Qmin/Qmax = (100%-25%)/(100%-10%) = 83%).

Note that for the future scenarios the time span in which the water heats up as a result of heat inputs between Basel and Worms is similar to the reference situation. However, the subsequent cooling in the Middle Rhine between Worms and Köln occurs faster in the future scenarios. This is visible in Figure 4-1, where the slope of the longitudinal profile (°C/km) is steeper for the near future compared to the reference and subsequently steeper for the far future compared to the near future. The stronger cooling over the same river stretch with the same heat input(s) is caused by the higher future water temperature. Physics dictate that the cooling of excess heat is faster at higher water temperatures. This is in line with the theory (Sweers 1976) and with observations made by ICPR (ICPR 2013a).

Natural variations in climate and river discharge lead to significant variation in water temperatures. Table 4-1 shows such variation in comparison to the reference period by means ofthe 90-percentile value which is roughly 2ºC higher than the average. The monthly average for August 2003 is more than 3ºC warmer than the 10-year August average. As August 2003 values roughly correspond with the results of the future simulation we can state that the extreme conditions experienced in August 2003 may serve as a model for the average summer situation in the far future (2071–2100).

Table 4-1: Simulation result for Ref50 and FF+Qmax (presented in Figure 4-1) compared to alternative characterisations of the reference period: the 90-percentile value for Augusts in 2000-2010 and the maximum monthly average for August 2003

		Basel	Worms	Köln	Lobith
Ref50: average Augusts 2001-2010	T (ºC)	20.5	22.5	22.6	22.7
Ref50: 90-percentile Augusts 2001-2010	T (ºC)	22.4	24.1	24.6	25.3
Ref50: average August 2003[11]	T (ºC)	23.8	26.5	25.6	25.5
FF+Qmax: average Augusts 2001-2010	T (ºC)	24.3	26.3	26.1	26.0

[11] Ref50 simulation results are not necessarily equal to the measured water temperatures (not shown in this table) as Ref50 does not use actual heat discharges. From the heat discharge analysis (3.2.1) it follows that the actual heat input in August 2003 is 34% of the permitted discharge. The difference with the assumed 50% in Ref50 amounts to 2800 MW (upstream Lobith). For example, at the average August 2003 river flow at Lobith (1013 m^3/s), which is significantly lower than the average flow of the reference period 2001-2010 (2264 m^3/s) and the average river flow corresponding with the scenario FF-Qmax (2038 m^3/s) and scenario FF-Qmin (1698 m^3/s), this amount of heat corresponds to an overestimation of the water temperature of 0.5-0.7ºC.

4.1.2 Summary statistics (tabular results)

Table 4.2 shows the results (water temperature) of the simulations as a table for selected stations along the Rhine together with the change in water temperature relative to the reference run (Ref50). The difference between Ref50 and Ref0 is the yearly averaged contribution of heat inputs. Appendix A shows data for more locations.

Table 4-2: Water temperature (T, °C) and difference from Ref50 in water temperature (Δ T, °C) statistics (average of yearly minimum, mean, maximum for 2001–2010) at selected locations simulated by LARSIM (Worms) and SOBEK (Koblenz, Lobith).

Location	Data	Ref0	Ref50	NF+ Qmax	NF+ Qmin	FF+ Qmax	FF+ Qmin
Worms	Average of yearly mean T	13.1	14.3	15.0	15.5	17.3	17.7
	Average of yearly minimum T	2.1	3.6	4.1	4.3	5.3	5.6
	Average of yearly maximum T	24.5	25.7	26.6	27.1	28.9	29.4
	Average of yearly mean ΔT	-1.1	0.0	0.8	1.2	3.0	3.5
	Average of yearly minimum ΔT	-1.5	0.0	0.5	0.7	1.7	2.0
	Average of yearly maximum ΔT	-1.1	0.0	0.9	1.4	3.2	3.7
Koblenz	Average of yearly mean T	13.0	14.2	15.0	15.3	17.1	17.3
	Average of yearly minimum T	1.5	3.1	3.5	3.7	4.6	4.8
	Average of yearly maximum T	24.9	26.1	26.8	27.3	29.1	29.4
	Average of yearly meanΔT	-1.2	0.0	0.8	1.1	2.9	3.2
	Average of yearly minimum ΔT	-1.6	0.0	0.4	0.5	1.5	1.7
	Average of yearly maximum ΔT	-1.2	0.0	0.7	1.2	3.0	3.3
Lobith	Average of yearly mean T	12.7	13.9	14.7	14.9	16.7	16.8
	Average of yearly minimum T	1.1	2.7	3.2	3.3	4.3	4.5
	Average of yearly maximum T	24.6	25.8	26.6	26.9	28.8	28.9
	Average of yearly meanΔT	-1.2	0.0	0.8	1.0	2.8	2.9
	Average of yearly minimum ΔT	-1.5	0.0	0.6	0.7	1.7	1.8
	Average of yearly maximum ΔT	-1.2	0.0	0.8	1.1	3.0	3.1

4.1.3 Exceeding frequency standards

Living organisms function only within a certain temperature range; outside this range activities such as reproduction are hampered. The exceeding frequencies of the water temperature for three critical values, viz. 25°C, 28°C and 3°C, are presented here. Temperatures above 25°C cause stress in flora and fauna; for example, if fish are exposed for a longer period to temperatures above 25°C, their life expectancy decreases. For salmonidwaters the temperature limit is even 21.5°C (see the directive on the quality of freshwater needing protection or improvement in order to support fish life 2006/44/EC). 28°C is the limit for cyprinid waters and must be obeyed. The 3°C limit

was analysed for ecological reasons such as the distribution of neozoa and the spawning of fish (ICPR 2009).

Figure 4-2 shows the average number of days per year on which the water temperature exceeds 25°C for a selected number of locations along the Rhine. The average number of days per year is calculated from the number of days per individual year. As some years are extremely warm (2003) and some do not exceed the 25°C limit at all (e.g. 2007), the spread in the average number of days is fairly large. Figure 4-2 shows deviation bars representing the tolerance interval covering 80% of the time, in other words for 8 out of 10 years the exceeding frequency falls within this range, in 20% of the time outside this range. For example, in the reference situation (Ref50) the 25°C standard is exceeded 11 times per year on average at Worms. The tolerance interval shown in Figure 4-2 is 0 to 30 days per year. In 2006 the 25°C limit was exceeded 28 times, in the extreme year 2003 even 45 times (this is outside the tolerance interval).

In the near future runs, the number of days exceeding 25°C increases; for the low discharge run (NF+Qmin) the number of days in excess of 25°C roughly doubles. Given the large variation over the years, there will still be some years in the near future without any exceedance of the 25°C standard (based on 2007). In the extreme years in the near future (based on 2003) the summer period exceeding 25°C will last up to at least 10 weeks (48-78 days) for the larger part of the Rhine.
In the far future the number of days with water temperatures exceeding 25°C strongly increases. For the low discharge run (FF+Qmin) the number of days in excess of 25°C increases approximately by a factor of five and more. Bars in Figure 4-2 indicate the range caused by natural variation over the years, the size of the bars covers 80%[12] of the years, in 10% of the years the number of days above 25°C is larger than the highest value of the range indicated (e.g. at Worms in the far future, FF+Qmin, excess temperature will occur on 100 days per year). In the near future the lowest value of the range is zero, indicating that in the near future there are still years where no exceedances of the 25°C standard takes place. In the far future this will be extremely rare.

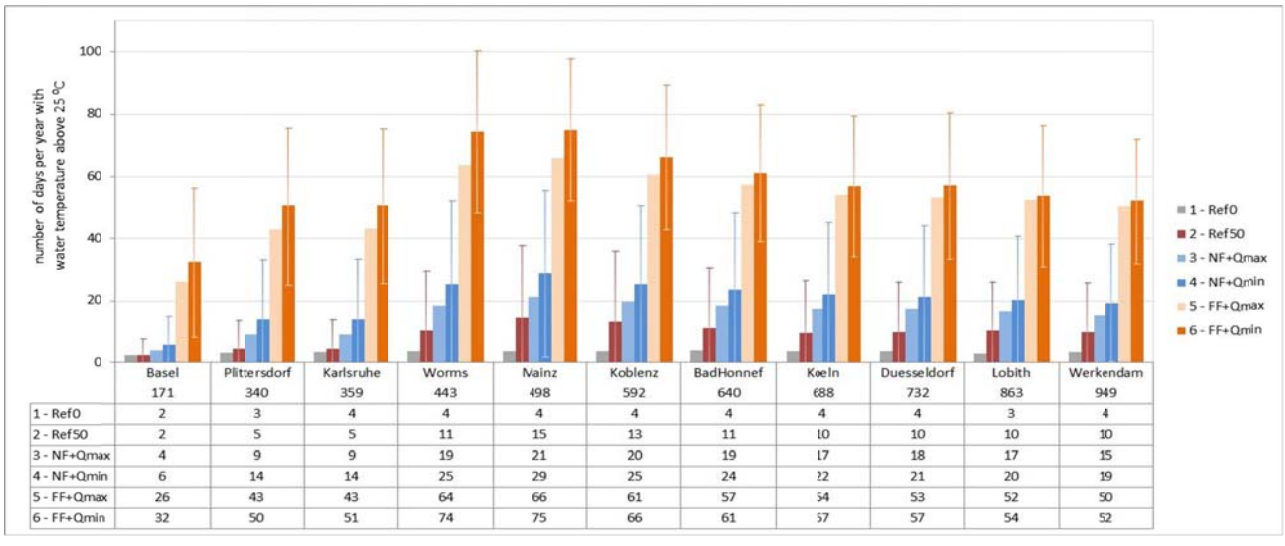

	Basel 171	Plittersdorf 340	Karlsruhe 359	Worms 443	Mainz 498	Koblenz 592	BadHonnef 640	Koeln 688	Duesseldorf 732	Lobith 863	Werkendam 949
1 - Ref0	2	3	4	4	4	4	4	4	4	3	4
2 - Ref50	2	5	5	11	15	13	11	10	10	10	10
3 - NF+Qmax	4	9	9	19	21	20	19	17	18	17	15
4 - NF+Qmin	6	14	14	25	29	25	24	22	21	20	19
5 - FF+Qmax	26	43	43	64	66	61	57	54	53	52	50
6 - FF+Qmin	32	50	51	74	75	66	61	57	57	54	52

Figure 4-2: Average number of days per year with water temperatures above 25°C along the Rhine for six scenarios. Results of LARSIM (Basel-Worms) and SOBEK (downstream of Worms). Deviation bars cover 80% of the variation in the

[12] The tolerance interval for sample averages (assuming a normal distribution) is calculated from $\mu \pm n\sigma$ using n equal to 1.28, in 20% of the cases the sample average is outside this range.

number of days above 25°C for a 10-yearperiod (shown for Ref50, NF+Qmin and FF+Qmin only).

In the far future, the water temperature in summer will be above 25°C during a large part of the summer period (up to 10 weeks). For the far future scenarios a higher water quality limit of 28°C is evaluated additionally.

Figure 4-3 shows that in the far future, exceedances of the 28°C limit occur in the Middle Rhine with an average frequency of 10 to 20 times per year, a similar frequency to that which occurs for the 25°C limit in the reference situation (Ref50).

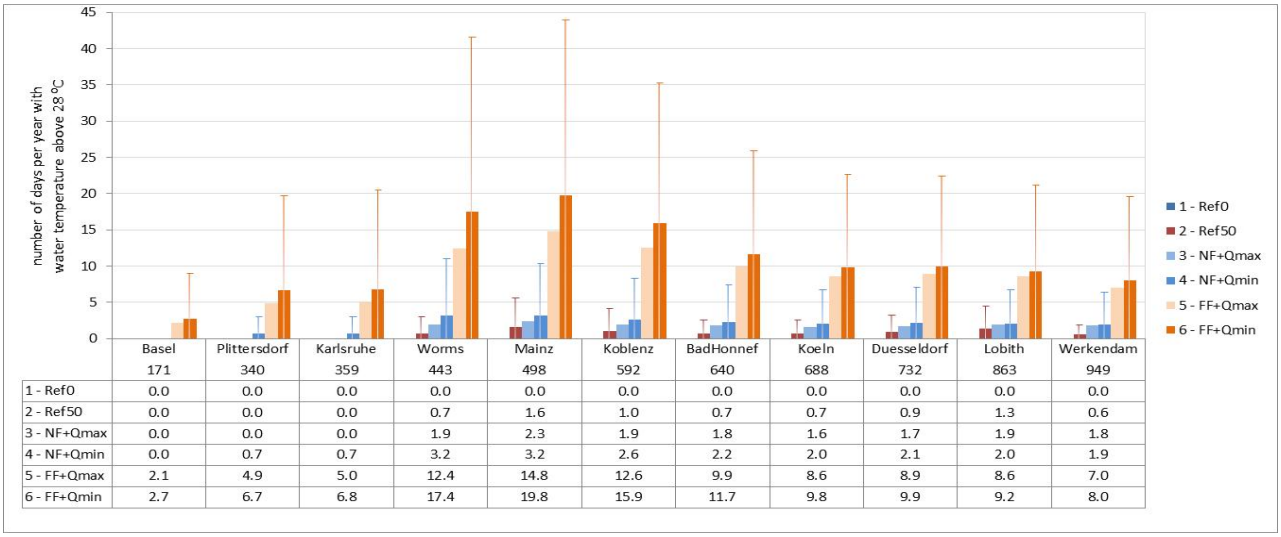

	Basel	Plittersdorf	Karlsruhe	Worms	Mainz	Koblenz	BadHonnef	Koeln	Duesseldorf	Lobith	Werkendam
	171	340	359	443	498	592	640	688	732	863	949
1 - Ref0	0.0	0.0	0.0	0.0	0.0	0.0	0.0	0.0	0.0	0.0	0.0
2 - Ref50	0.0	0.0	0.0	0.7	1.6	1.0	0.7	0.7	0.9	1.3	0.6
3 - NF+Qmax	0.0	0.0	0.0	1.9	2.3	1.9	1.8	1.6	1.7	1.9	1.8
4 - NF+Qmin	0.0	0.7	0.7	3.2	3.2	2.6	2.2	2.0	2.1	2.0	1.9
5 - FF+Qmax	2.1	4.9	5.0	12.4	14.8	12.6	9.9	8.6	8.9	8.6	7.0
6 - FF+Qmin	2.7	6.7	6.8	17.4	19.8	15.9	11.7	9.8	9.9	9.2	8.0

Figure 4-3: Average number of days per year with water temperature above 28°C along the Rhine for six scenarios. Results of LARSIM (Basel-Worms) and SOBEK (downstream of Worms). Deviation bars cover 80% of the variation in the number of days above 28°C for a 10-year-period (shown for Ref50, NF+Qmin and FF+Qmin only).

Figure 4-4 shows the average number of days per year on which the water temperature is below 3°C for a selected number of locations along the Rhine. The reference situation (Ref50) clearly shows a minimum of the number of "cold" days at Worms. This minimum is a consequence of the location of the input of thermal discharges along the Rhine. Compared to the natural situation without heat inputs (Ref0), the yearly averaged number of days with water temperature lower than 3°C declines from 10 days to 1 day around Worms in the reference situation (Ref50) and zero days in the near and far future.

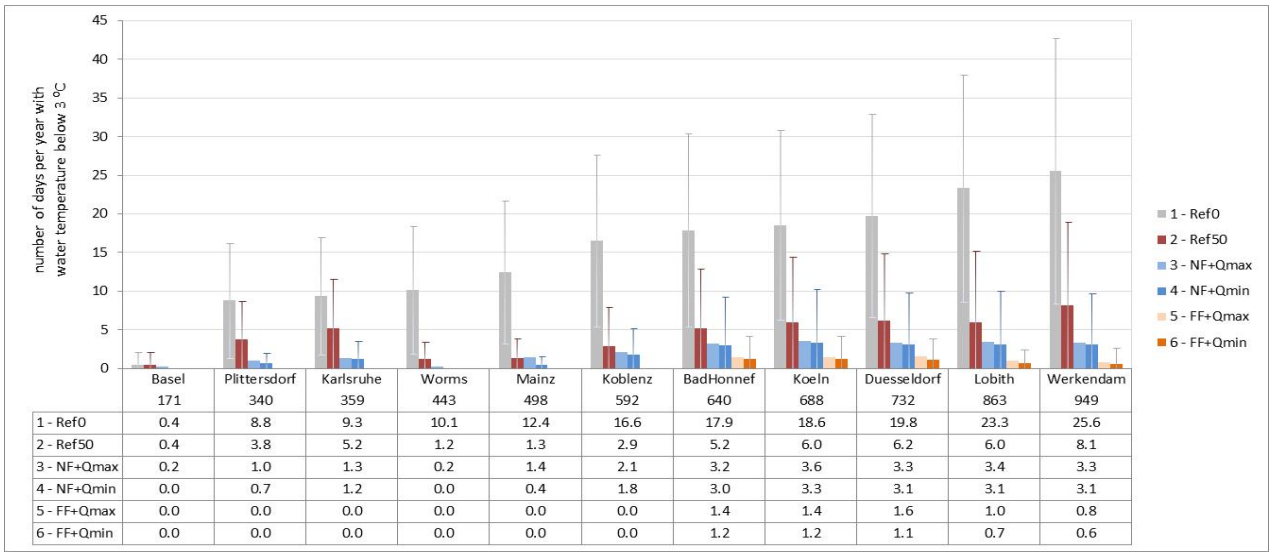

	Basel	Plittersdorf	Karlsruhe	Worms	Mainz	Koblenz	BadHonnef	Koeln	Duesseldorf	Lobith	Werkendam
	171	340	359	443	498	592	640	688	732	863	949
1 - Ref0	0.4	8.8	9.3	10.1	12.4	16.6	17.9	18.6	19.8	23.3	25.6
2 - Ref50	0.4	3.8	5.2	1.2	1.3	2.9	5.2	6.0	6.2	6.0	8.1
3 - NF+Qmax	0.2	1.0	1.3	0.2	1.4	2.1	3.2	3.6	3.3	3.4	3.3
4 - NF+Qmin	0.0	0.7	1.2	0.0	0.4	1.8	3.0	3.3	3.1	3.1	3.1
5 - FF+Qmax	0.0	0.0	0.0	0.0	0.0	0.0	1.4	1.4	1.6	1.0	0.8
6 - FF+Qmin	0.0	0.0	0.0	0.0	0.0	0.0	1.2	1.2	1.1	0.7	0.6

Figure 4-4: Average number of days per year with water temperature below 3°C along the Rhine for six scenarios. Results of LARSIM (Basel-Worms) and SOBEK (downstream of Worms).Deviation bars cover 80% of the yearly variation in the number of days below 3°C for a 10-year-period(shown for Ref50, NF+Qmin and FF+Qmin only).

For those Rhine stretches that are less influenced by thermal heat inputs up to Lobith, the number of days with water temperatures below 3°C in the reference situation (Ref50) ranges from 4 to 6; this number declines to 1-3 in the near and to 0-1 in the far future.

The reduction in the number of days with water temperatures below 3°C going from the natural (Ref0) to the reference situation (Ref50) is relatively large compared to the further reduction in the future as a result of the assumed climate change. Heat discharges in winter have a significant impact on the statistic evaluated. This may be a result of the fact that the cooling of excess heat is slower at lower water temperatures (Sweers 1976).

4.2 Comparison of the available models

In this paragraph the scenario results for the Rhine, running from Basel to the river delta in the Netherlands, are presented. The results are based on simulations by three models that were applied in this study (LARSIM, QSim and SOBEK). See Fig. 3-1 for the river stretches covered by the models. Table 4-3 gives an overview of the model coverage for selected stations presented in this paragraph. The table shows that results of three models are notably available for the Middle Rhine (Karlsruhe-Köln). Further downstream, up to Lobith, the results presented in this chapter are based on two models. QSim starts in Karlsruhe and SOBEK starts in Worms, both using the water temperature simulated by LARSIM for all scenarios.

These additional results for overlapping stretches of the river Rhine indicate the spread in the model predictions, which can be attributed to the intrinsic properties of the individual models.

Table 4-3: Overview of water temperature stations along the Rhine and the availability of model results for these stations. Dots indicate the connection of QSim and SOBEK to LARSIM, and multiple model results are available for the greyed stations.

Location	Model			Number of Models
Basel	LARSIM			1
Plittersdorf	LARSIM			1
Karlsruhe	LARSIM			1
Worms	LARSIM	QSim		2
Mainz	LARSIM	QSim	SOBEK	3
Koblenz	LARSIM	QSim	SOBEK	3
Bad Honnef	LARSIM	QSim	SOBEK	3
Köln	LARSIM	QSim	SOBEK	3
Düsseldorf		QSim	SOBEK	2
Lobith		QSim	SOBEK	2
Werkendam			SOBEK	1

4.2.1 Temperature profile of the Rhine

Figure 4-5 shows the development of the average August water temperature in the Rhine, predicted by three models. Upstream of Worms, QSim and LARSIM show nearly the same result for all simulations.

QSim starts at Karlsruhe and SOBEK at Worms with the data from LARSIM. In the Middle Rhine stretch (Worms-Köln) the three models show a strong similarity to the natural situation (Ref0): SOBEK and QSim are more or less the same, LARSIM slightly (0.1°C) warmer. For the reference run including heat discharges (Ref50) the results are still similar but LARSIM shows somewhat stronger cooling in comparison with SOBEK, resulting in slightly colder water (0.1°C) at Köln. QSim shows the strongest cooling, resulting in the coolest water at Köln (0.5°C lower than SOBEK).

In section 4.1 the conclusion from the slope of the longitudinal water temperature profile (°C/km) is that, for LARSIM and SOBEK, the cooling in the Middle Rhine is stronger for future scenarios when the water temperature is higher. For QSim the slope appears equally high in all scenarios.

Downstream of Köln there is a difference between SOBEK and QSim for the natural situation (Ref0), QSim being approximately 0.35°C cooler than SOBEK at Lobith. For the reference run including heat discharges (Ref50), the difference between the two models increases to approximately 0.7°C at Lobith. Earlier, SOBEK and QSim also showed fairly strong differences in the cooling of heat discharges (Deltares 2011).

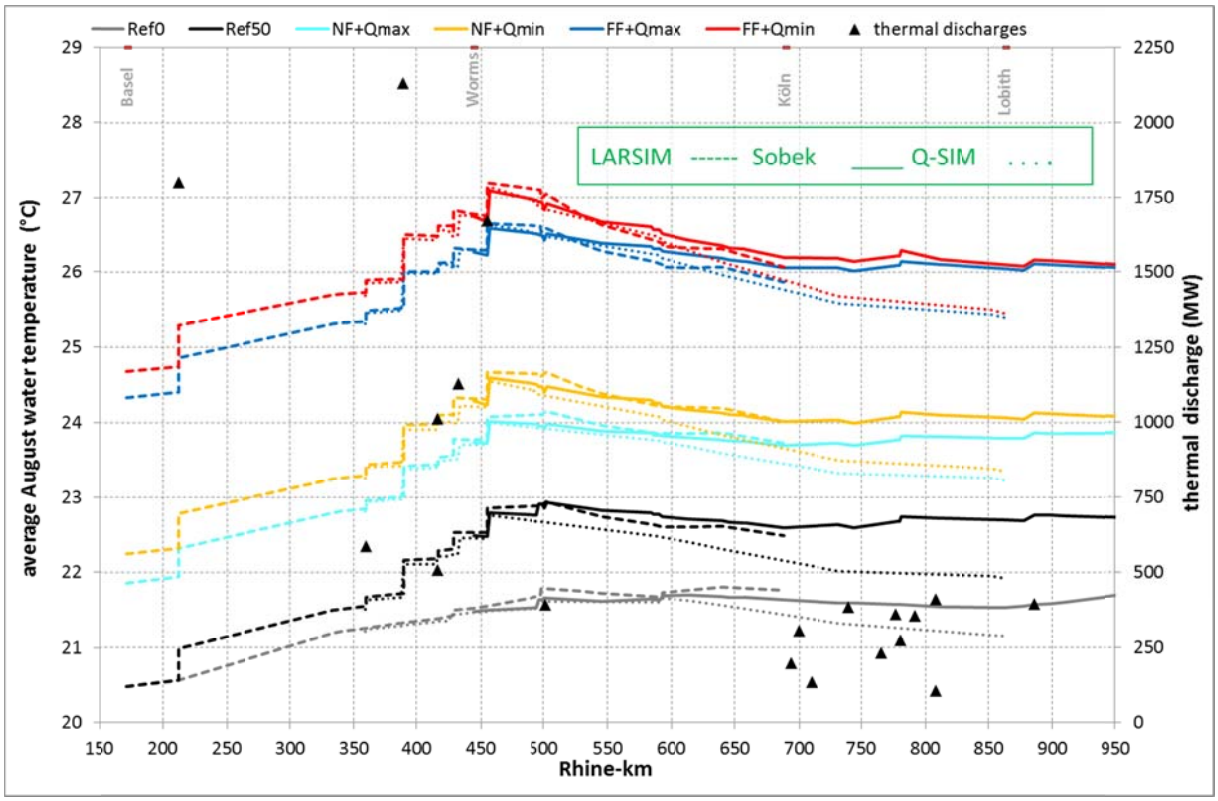

Figure 4-5: Longitudinal profile in the Rhine (Basel-Delta) of average August water temperature (°C) for six scenarios simulated by LARSIM (Basel-Köln), SOBEK (Worms-Werkendam) and QSim (Karlsruhe-Lobith)

4.2.2 Summary statistics (tabular results)

Table 4-4 shows average, minimum and maximum water temperature at Koblenz as simulated by the three models. Data for other stations may be found in Appendix A. In general the models show good agreement, the range between the lowest and highest prediction of the average temperature is less than 0.6 ºC. Differences in the ΔT (temperature change relative to Ref50) are smaller, only 0.3ºC in the far future. The models deviate more in their prediction of the minimum temperature in the reference situation (maximum deviation 0.7ºC).

Table 4-4: Statistics (minimum, mean, maximum for 2001–2010) of water temperature (absolute T and ΔT compared to Ref50) at Koblenz simulated by LARSIM, QSim and SOBEK)

Data	Model	Ref0	Ref50	NF+Qmax	NF+Qmin	FF+Qmax	FF+Qmin
Average of yearly mean T	LARSIM	13.0	14.0	14.8	15.1	17.0	17.3
	QSim	12.8	13.7	14.5	14.7	16.5	16.7
	SOBEK	13.0	14.2	15.0	15.3	17.1	17.3
Average of yearly mean ΔT	LARSIM	-1.0		0.9	1.1	3.0	3.3
	QSim	-1.0		0.8	1.0	2.8	3.0
	SOBEK	-1.2		0.8	1.1	2.9	3.2
Average of yearly minimum T	LARSIM	1.4	2.7	3.4	3.5	4.6	4.9
	QSim	2.0	3.4	3.8	3.8	4.7	4.8
	SOBEK	1.5	3.1	3.5	3.7	4.6	4.8
Average of yearly minimum ΔT	LARSIM	-1.3		0.7	0.8	2.0	2.2
	QSim	-1.3		0.4	0.5	1.4	1.4
	SOBEK	-1.6		0.4	0.5	1.5	1.7
Average of yearly maximum T	LARSIM	24.5	25.5	26.4	26.8	28.5	28.8
	QSim	24.8	25.7	26.7	27.0	29.0	29.3
	SOBEK	24.9	26.1	26.8	27.3	29.1	29.4
Average of yearly maximum ΔT	LARSIM	-1.0		0.9	1.2	3.0	3.3
	QSim	-1.0		0.9	1.3	3.3	3.6
	SOBEK	-1.2		0.7	1.2	3.0	3.3

4.2.3 Exceeding frequency standards

Figure 4-6 shows the number of days per year on which the water temperature exceeds 25°C for six stations, where results based on two or more model results are available. The deviation bars indicate a 95% confidence interval for the number of days exceeding 25ºC. The graph implies that the spread in results caused by the fact that different models are averaged is relatively small compared to the natural variation in the number of days exceeding 25ºC over the years (see Figure 4-2). At Worms the two models (QSim and LARSIM) show very similar values for the number of days exceeding 25ºC and thus show very small confidence intervals for all but the far future scenarios. For the far future, the interval is relatively large at Worms. This may be the combined effect of LARSIM simulating the highest water temperatures at the model boundary in the far future (see 3.3.4) and QSim simulating the strongest cooling of the excess heat (see 4.2). Going downstream from Worms, the spread in the models gradually increases.

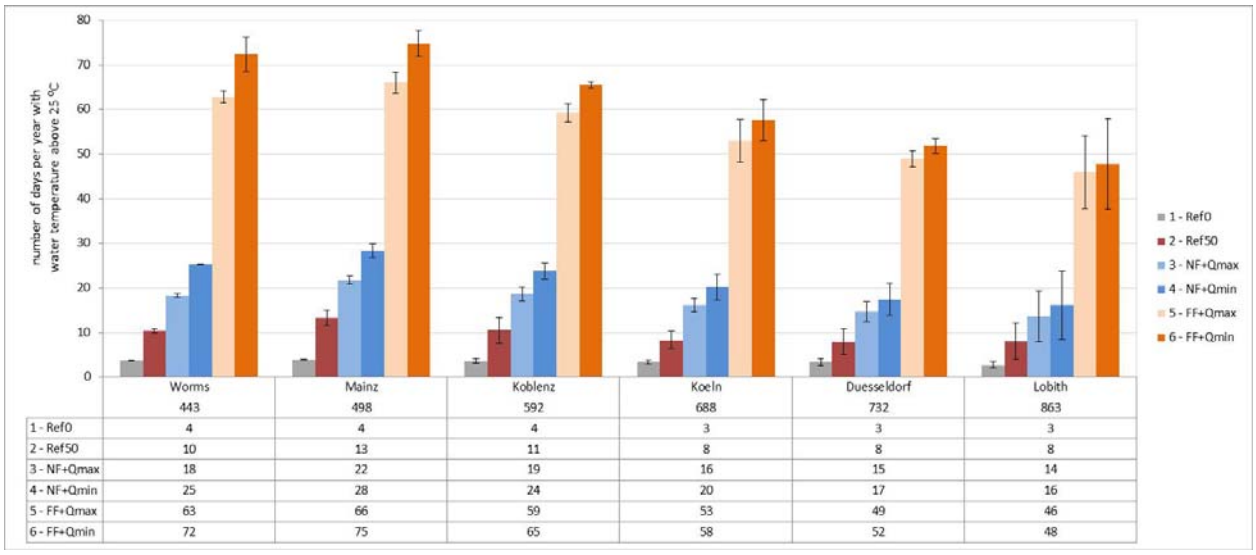

	Worms	Mainz	Koblenz	Koeln	Duesseldorf	Lobith
	443	498	592	688	732	863
1 - Ref0	4	4	4	3	3	3
2 - Ref50	10	13	11	8	8	8
3 - NF+Qmax	18	22	19	16	15	14
4 - NF+Qmin	25	28	24	20	17	16
5 - FF+Qmax	63	66	59	53	49	46
6 - FF+Qmin	72	75	65	58	52	48

Figure 4-6: Number of days per year with water temperature above 25°C along the Rhine based on references (R50) 2001–2010 and for future scenarios.Combined results of LARSIM, QSim and SOBEK.The deviation bars indicate 95% confidence interval for the different models.

4.3 Conclusions

The heat discharge inventory carried out in this study shows that actual heat inputs in August 2003 were 34% of the permitted values. For the full reference period 2001–2010, the average was 50%, which is used as the basis for the scenarios (50% of the 2010 permitted heat discharge).

The three models LARSIM, SOBEK and QSim are successfully validated against measurements. They proved to be adequate for future predictions for which accuracy suffices in the order of 0.5ºC.

The effects of assumed climate change on water temperature are as different as the different model approaches, notably for the model boundaries. However, the variation between the models is small, especially when compared to the natural annual variations in water temperature on the one hand (ca. 1 to 30°C) and the prognosis of the climate change effects (1.5 to 4ºC) on the other hand.

The assumed climate change produces an increase in summer water temperature of 1.5ºC in the near future and over 3.0ºC in the far future. Approximately 2/3 of the assumed increase in air temperature is transmitted in a water temperature increase (so air temperature cannot be translated 1:1 into water temperature). With respect to absolute temperatures, the natural inter-annual variation must be considered.

The extreme conditions experienced in August 2003 may serve as a model for the average summer situation in the far future (2071–2100). The number of days exceeding 25ºC is predicted to double on average in the near future. In the far future the exceeding frequency of 28ºC is simulated to be similar to the current exceeding frequency of 25ºC.

The number of days with water temperatures below 3ºC in the reference situation (Ref50) is small compared to the natural situation (Ref0) as a result of heat inputs. The predicted effect of the assumed climate change on winter water temperatures is

therefore limited, as there are already today not many days below 3ºC in the reference situation which could be further reduced in the future scenarios.

The fate of anthropogenic heat inputs as predicted by QSim deviates from the predictions by LARSIM and SOBEK. It is recommended to compare specific aspects of the models with respect to the cooling of thermal heat inputs. The processes of evaporation, back radiation and conduction determine heat exchange coefficients across the air-water interface and thus the dissipation rate of excess heat input. In addition, the process for calculating future water temperatures for the model boundaries differs for LARSIM compared to QSim and SOBEK. A comparison of the individual heat fluxes and the approaches for the model boundary calculations is recommended.

In this study the period 2001–2010 was used as a reference to simulate the effect of the assumed climate change on Rhine water temperatures in the near and far future. The reference period 2001–2010 is characterized by strong variations in water temperature and river discharge. This 10-yearperiod is a sound basis for the modelling of the future changes in water temperature, as different meteorological and hydrological conditions were covered.

The main focus of this study was to identify the range of change in water temperature due to the assumed climate change. The study shows that all three models –LARSIM, QSim and SOBEK – are suitable for modelling the temperature regime in the Rhine and are available for further applications, such as an investigation into the effect of the bandwidth and not a mean value (delta change approach) in climate change.

5. References

Becker, A.; V. Kirchesch; H.Z. Baumert; H. Fischer & A. Schöl (2010): Modelling the effects of thermal stratification on the oxygen budget of an impounded river. River Research and Applications 26 (5): 572-588.

BfG (2005): Hydrological modelling in the river Rhine basin part III - daily HBV model for the Rhine basin. Eberle, M.;Buiteveld, H.; Wilke, K.andKrahe, P.; RIZA and BfG, Koblenz, Germany, BfG-report 1451.

BfG (2013): Klimaänderungsvektoren als Grundlage für die Modellierung von Wassertemperaturänderungen im Rheingebiet. -Technische Dokumentation. Enno Nilson, Peter Krahe& Klaus Görgen. Bundesanstalt für Gewässerkunde und Meteorologisches Institut der Universität Bonn, 23 p.

Bremicker, M. (2000): Das Wasserhaushaltsmodell LARSIM – Modellgrundlagen und Anwendungsbeispiele. Freiburger Schriften zur Hydrologie, Band 11. Institut für Hydrologie der Universität Freiburg.

Dalton, John (1803): "Versuche über die Verdunstung." Annalen der Physik 15.10: 121-143.

Deltares (2011): Watertemperature Rhine. Contribution of cooling water to the ambient water temperature: measurements and models. Author: Boderie,Deltares report 1203156.

Evans, E.C.; G.R. McGregor; G.E.Petts (1998): River energy budgets with special reference to river bed processes. Hydrological processes, 12, 575-595.

Gill, A.E. (1982): Atmosphere-ocean dynamics, Academic press.

Haag, I. & Luce, A. (2008): LARSIM: an integrated water-balance and heat-balance model to simulate and predict stream water temperatures. Hydrological Processes 22, 1046-1056.

Haag, I.; Luce, A.; Badde, U. (2005): Ein operationelles Vorhersagemodell für die Wassertemperatur im Neckar. Wasserwirtschaft, 95(7/8), 45 – 51.

Hardenbicker, P. (2013): Phytoplankton dynamics in two large rivers: Long-term trends, longitudinal dynamics and potential impacts of assumed climate change. Doctoral Dissertation, Technical University Dresden.

ICPR (2004): Wärmebelastung der Gewässer im Sommer 2003. Zusammenfassung der nationalen Situationsberichte. ICPR-report 142.

ICPR (2009): Analysis of the state of knowledge on climate changes so far and on the impact of climate change on the water regime in the Rhine watershed - Literature evaluation. ICPR-report174.

ICPR (2011): Study of scenarios for the discharge regime of the Rhine. ICPR-report 188.

ICPR (2013a): Presentation of the development of the Rhine water temperature on the basis of validated temperature measurements from 1978 until 2011. ICPR-report 209.

ICPR (2013b): Present state of knowledge on possible consequences of changes of the discharge pattern and water temperature on the Rhine ecosystem and possible perspectives for action. ICPR-report 204.

Kasten, F (1989): Strahlungsaustausch zwischen Oberflächen und Atmosphäre. VDI Berichte 721.

Kremer, M. &Brahmer, G. (2012): Simulation und Vorhersage von Wassertemperaturen an hessischen Fließgewässern. Jahresbericht 2012 des Hessischen Landesamtes für Umwelt und Geologie, Wiesbaden, 31 - 38.

Lane, A. (1989): The heatbalanceofthe North Sea. Tech. Rep. 8, Proudman Oceanographic Laboratory.251, 261

LAWA (1991): Grundlagen für die Beurteilung von Kühlwassereinleitungen in Gewässer. Herausgegeben von der Länderarbeitsgemeinschaft Wasser – Ausgearbeitet von der LAWA-Arbeitsgruppe – Wärmebelastung der Gewässer – Erich Schmidt Verlag, Berlin: 119 Seiten.

LfU (2005): Operationelles Wärmemodell für den Neckar zwischen Plochingen und Mannheim. Ing.-Büro Dr. Karl Ludwig, Karlsruhe, im Auftrag der Landesanstalt für Umweltschutz, Baden-Württemberg (unveröffentlicht).

Mohseni O. & H.G. Stefan (1999): Stream temperature/air temperature relationship: a physical interpretation. – Journal of Hydrology, 218, 128-141.

Octavia, K. A. H.; G. H. Jirka and D. R. F. Harleman (1977): Vertical Heat Transport Mechanisms in Lakes and Reservoirs. Tech. Rep. 22, Massachusetts Institute of Technology. 251, 254, 255, 260

Oppermann, R. (1989): Eindimensionale Simulation allmählich veränderlicher instationärer Fließvorgänge in Gewässernetzen. Verlag für Bauwesen, Berlin.

Oppermann, R. (2010): Das Programmsystem HYDRAX 5.0 - Mathematisches Modell und Datenschnittstellen. Auftraggeber: Ingenieurbüro für Wasser und Umwelt, Berlin.

Prescott, J.A. (1940): Evaporation fromwatersurface in relationto solar radiation. Trans. Royal Society Australia 46, 114-118.

Postma, L.; Boderie, P.M.A.; Gils, J.A.G. van; Beek, J.K.L. van. Component Software Systems for Surface Water Simulation in Sloot et al. (Eds): ICCS 2003, LNCS 2657, pp 649-658, 2003; Springer- Verlag Berlin Heidelberg

Quiel, K.; A. Becker; A. Schöl; V. Kirchesch& H. Fischer (2011): Influence of global change on phytoplankton and nutrient cycling in the Elbe River. Regional Environmental Change 11: 405,421.

Sweers, H.E. (1976): A monogram to estimate the heat exchange coefficient at the air-water interface as a function of wind speed and temperature; a critical survey of some literature. Journal of Hydrology, vol. 30.

WMO (World Meteorological Organisation) (1966): Climatic change. Geneva, Tech. Note 79.

Appendix A. Tables of simulation results

Table A.1: Water temperature (T, °C) (minimum, mean, maximum) for six scenarios at selected locations simulated by LARSIM (Basel, Karlsruhe, Worms) and SOBEK (Mainz, Koblenz, Lobith, Delta)

Location	Data	Ref0	Ref50	NF+Qmax	NF+Qmin	FF+Qmax	FF+Qmin
Basel	Average of yearly mean T	12.9	12.9	13.7	14.1	15.9	16.2
	Average of yearly minimum T	3.7	3.7	3.9	4.2	4.8	5.1
	Average of yearly maximum T	24.2	24.2	25.0	25.4	27.0	27.4
Worms	Average of yearly mean T	13.1	14.3	15.0	15.5	17.3	17.7
	Average of yearly minimum T	2.1	3.6	4.1	4.3	5.3	5.6
	Average of yearly maximum T	24.5	25.7	26.6	27.1	28.9	29.4
Mainz	Average of yearly mean T	13.1	14.4	15.2	15.6	17.4	17.8
	Average of yearly minimum T	1.9	3.6	3.9	4.1	5.1	5.4
	Average of yearly maximum T	24.8	26.2	26.9	27.4	29.2	29.7
Koblenz	Average of yearly mean T	13.0	14.2	15.0	15.3	17.1	17.3
	Average of yearly minimum T	1.5	3.1	3.5	3.7	4.6	4.8
	Average of yearly maximum T	24.9	26.1	26.8	27.3	29.1	29.4
Lobith	Average of yearly mean T	12.7	13.9	14.7	14.9	16.7	16.8
	Average of yearly minimum T	1.1	2.7	3.2	3.3	4.3	4.5
	Average of yearly maximum T	24.6	25.8	26.6	26.9	28.8	28.9
Werken-dam	Average of yearly mean T	12.7	13.8	14.7	14.8	16.6	16.6
	Average of yearly minimum T	1.1	2.6	3.2	3.3	4.4	4.5
	Average of yearly maximum T	24.5	25.6	26.4	26.7	28.6	28.8

Table A.2: Difference in water temperature (Δ T, °C) (minimum, mean, maximum) for five scenarios relative to the reference situation (Ref50) at selected locations simulated by LARSIM (Basel, Karlsruhe, Worms) and SOBEK (Mainz, Koblenz, Lobith, Delta).

Location	Data	Ref0	Ref50	NF+Qmax	NF+Qmin	FF+Qmax	FF+Qmin
Basel	Average of yearly mean ΔT	0.0	0.0	0.8	1.2	2.9	3.3
	Average of yearly minimum ΔT	0.0	0.0	0.2	0.5	1.1	1.5
	Average of yearly maximum ΔT	0.0	0.0	0.9	1.3	2.8	3.2
Karls-ruhe	Average of yearly mean ΔT	-0.3	0.0	0.9	1.2	3.0	3.4
	Average of yearly minimum ΔT	-0.4	0.0	0.6	0.7	1.7	2.0
	Average of yearly maximum ΔT	-0.3	0.0	0.9	1.3	3.1	3.5
Worms	Average of yearly mean ΔT	-1.1	0.0	0.8	1.2	3.0	3.5
	Average of yearly minimum ΔT	-1.5	0.0	0.5	0.7	1.7	2.0
	Average of yearly maximum ΔT	-1.1	0.0	0.9	1.4	3.2	3.7
Mainz	Average of yearly mean ΔT	-1.3	0.0	0.8	1.1	2.9	3.3
	Average of yearly minimum ΔT	-1.7	0.0	0.3	0.5	1.5	1.8
	Average of yearly maximum ΔT	-1.4	0.0	0.7	1.2	3.1	3.5
Koblenz	Average of yearly mean ΔT	-1.2	0.0	0.8	1.1	2.9	3.2
	Average of yearly minimum ΔT	-1.6	0.0	0.4	0.5	1.5	1.7
	Average of yearly maximum ΔT	-1.2	0.0	0.7	1.2	3.0	3.3
Lobith	Average of yearly mean ΔT	-1.2	0.0	0.8	1.0	2.8	2.9
	Average of yearly minimum ΔT	-1.5	0.0	0.6	0.7	1.7	1.8
	Average of yearly maximum ΔT	-1.2	0.0	0.8	1.1	3.0	3.1
Werken-dam	Average of yearly mean ΔT	-1.1	0.0	0.8	1.0	2.7	2.8
	Average of yearly minimum ΔT	-1.4	0.0	0.6	0.7	1.8	1.9
	Average of yearly maximum ΔT	-1.1	0.0	0.8	1.1	3.0	3.1

Table A.3: Water temperature (°C) (minimum, mean, maximum) at selected locations for six scenarios simulated by LARSIM, QSim and SOBEK.

Location	Data	Model	Ref0	Ref50	NF+ Qmax	NF+ Qmin	FF+ Qmax	FF+ Qmin
Mainz	Average of yearly mean T	LARSIM	13.1	14.3	15.1	15.5	17.3	17.7
		QSim	13.0	14.1	14.9	15.2	17.0	17.3
		SOBEK	13.1	14.4	15.2	15.6	17.4	17.8
	Average of yearly minimum T	LARSIM	1.9	3.4	3.9	4.1	5.1	5.4
		QSim	2.3	3.8	4.3	4.4	5.3	5.5
		SOBEK	1.9	3.6	3.9	4.1	5.1	5.4
	Average of yearly maximum T	LARSIM	24.8	26.0	26.8	27.3	29.1	29.5
		QSim	24.8	26.0	26.9	27.4	29.3	29.8
		SOBEK	24.8	26.2	26.9	27.4	29.2	29.7
Koblenz	Average of yearly mean T	LARSIM	13.0	14.0	14.8	15.1	17.0	17.3
		QSim	12.8	13.7	14.5	14.7	16.5	16.7
		SOBEK	13.0	14.2	15.0	15.3	17.1	17.3
	Average of yearly minimum T	LARSIM	1.4	2.7	3.4	3.5	4.6	4.9
		QSim	2.0	3.4	3.8	3.8	4.7	4.8
		SOBEK	1.5	3.1	3.5	3.7	4.6	4.8
	Average of yearly maximum T	LARSIM	24.5	25.5	26.4	26.8	28.5	28.8
		QSim	24.8	25.7	26.7	27.0	29.0	29.3
		SOBEK	24.9	26.1	26.8	27.3	29.1	29.4
Bad Honnef	Average of yearly mean T	LARSIM	13.0	13.8	14.7	15.0	16.9	17.1
		QSim	12.7	13.5	14.3	14.5	16.2	16.3
		SOBEK	12.9	14.0	14.8	15.0	16.8	17.0
	Average of yearly minimum T	LARSIM	1.5	2.5	3.2	3.3	4.5	4.7
		QSim	2.1	3.1	3.6	3.6	4.6	4.6
		SOBEK	1.3	2.7	3.2	3.3	4.3	4.4
	Average of yearly maximum T	LARSIM	24.6	25.5	26.4	26.7	28.4	28.6
		QSim	24.7	25.5	26.4	26.7	28.7	29.0
		SOBEK	24.9	26.0	26.7	27.1	28.9	29.1

Table A.4: Difference in water temperature (delta (Δ)T, °C) (minimum, mean, maximum) for five scenarios relative to the reference situation (Ref50) at selected locations simulated by LARSIM, QSim and SOBEK.

Location	Data	Model	Ref 0	Ref 50	NF+ max	NF+ Qmin	FF+ Qmax	FF+ Qmin
Mainz	Average of yearly mean ΔT	LARSIM	1.2	0.0	0.8	1.2	3.0	3.4
		QSim	1.1	0.0	0.8	1.1	2.9	3.2
		SOBEK	1.3	0.0	0.8	1.1	2.9	3.3
	Average of yearly minimum ΔT	LARSIM	1.5	0.0	0.5	0.7	1.7	2.1
		QSim	1.5	0.0	0.4	0.5	1.5	1.7
		SOBEK	1.7	0.0	0.3	0.5	1.5	1.8
	Average of yearly maximum ΔT	LARSIM	1.2	0.0	0.9	1.4	3.1	3.6
		QSim	1.2	0.0	0.9	1.4	3.3	3.8
		SOBEK	1.4	0.0	0.7	1.2	3.1	3.5
Koblenz	Average of yearly mean ΔT	LARSIM	1.0	0.0	0.9	1.1	3.0	3.3
		QSim	1.0	0.0	0.8	1.0	2.8	3.0
		SOBEK	1.2	0.0	0.8	1.1	2.9	3.2
	Average of yearly minimum ΔT	LARSIM	1.3	0.0	0.7	0.8	2.0	2.2
		QSim	1.3	0.0	0.4	0.5	1.4	1.4
		SOBEK	1.6	0.0	0.4	0.5	1.5	1.7
	Average of yearly maximum ΔT	LARSIM	1.0	0.0	0.9	1.2	3.0	3.3
		QSim	1.0	0.0	0.9	1.3	3.3	3.6
		SOBEK	1.2	0.0	0.7	1.2	3.0	3.3
Bad Honnef	Average of yearly average ΔT	LARSIM	0.8	0.0	0.9	1.1	3.0	3.3
		QSim	0.8	0.0	0.8	1.0	2.7	2.9
		SOBEK	1.0	0.0	0.8	1.1	2.9	3.0
	Average of yearly minimum ΔT	LARSIM	1.0	0.0	0.7	0.8	2.0	2.2
		QSim	1.0	0.0	0.5	0.5	1.4	1.5
		SOBEK	1.4	0.0	0.5	0.6	1.6	1.7
	Average of yearly maximum ΔT	LARSIM	0.9	0.0	0.9	1.2	2.9	3.2
		QSim	0.8	0.0	1.0	1.3	3.3	3.5
		SOBEK	1.1	0.0	0.7	1.1	3.0	3.2

Appendix B. Brief description of the LARSIM heat model

Fundamentals of the daily value-based LARSIM water temperature model

Overview of the LARSIM-WT water temperature model

The LARSIM model for simulating water temperature is an extension of the water balance model (WBM) LARSIM (Bremicker 2000). The modules integrated additionally into LARSIM for calculating water temperature are known as the temperature model (WTM) and the overall model is known as the water balance and temperature model (WBTM) (Haag et al. 2005, Haag & Luce 2008).

The WBTM is driven by the meteorological input data shown in Figure 1. The water balance forms the basis for the simulation of the water temperature. In the process, the accumulation and depletion of snow storage, interception and evapotranspiration, and the soil water balance are simulated with unchanged WBM modules, without calculating the water temperature (Figure 1). However, these processes are of no significance to the model used in this study, which covers exclusively the Rhine itself.

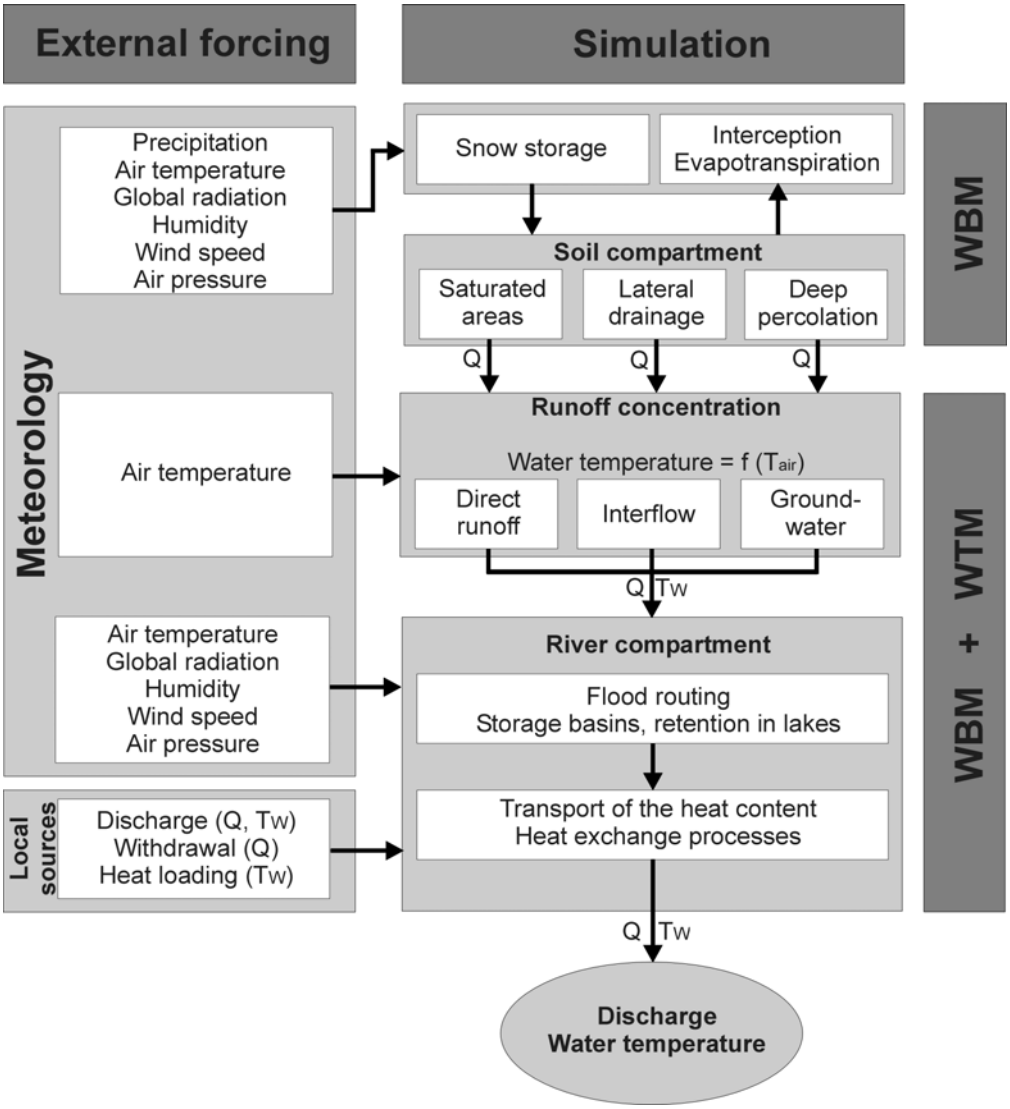

Figure 1: Model diagram of the LARSIM water balance and temperature model (WBTM)

In the simulation of the three areas of storage (runoff concentration) and the flood routing in the river compartments, the water temperature is also calculated. Here, along with factors of climactic influence, selective sources of heat in the form of heat loading capacity or discharges with defined temperatures as well as water withdrawal can also be considered. As a result of a WBTM simulation we receive the discharges and water temperatures in the running waters of the simulated catchment area.

Physically-based calculation of the water temperature

In the physically-based simulation the water temperatures of the discharge portions from the areas of storage are expressed as linear functions of the current air temperature in each case for direct runoff, interflow and groundwater. Using the slope and the intersect takes account of the fact that the temperature of the groundwater discharge roughly represents the long-term average of air temperature, while the direct runoff is influenced to a much greater degree by current air temperature due to its very brief length of stay in the catchment area. The position of the interflow is between these two (for details see LfU (2005)).

The subsequent transport to the river compartments is calculated with the one-dimensional advection-dispersion equation:

(Eq.1)
$$\frac{\partial T_W}{\partial t} + u \cdot \frac{\partial T_W}{\partial x} = E_x \cdot \frac{\partial^2 T_W}{\partial x^2} \pm S$$

The flow velocity (u) is produced by the discharge calculated with the WBM and the cross-section flowed through by water. The longitudinal dispersion coefficient (E_x) is estimated with the help of an empirical equation suggested by Fischer et al. (1977). The source-sink term (S) contains on the one hand the sum of the relevant heat exchange processes between the atmosphere and the riverbed. On the other hand it also captures local sources such as the heat discharge by thermal power plants.
With regard to the changes in temperature due to heat exchange with the environment, the processes illustrated in Figure 2 are considered in the source-sink term. Therefore, for the change rate of the water temperature as a result of heat exchange processes in the river compartment, the following equation is taken as a basis (for variable definition see Equation 2):

(Eq. 2)
$$\frac{dT_W}{dt} = \frac{R_K + R_L + H_F + H_L + R_{Sed}}{c_p \cdot \rho_W \cdot h}$$

The river depth (h) is expressed here as a function of the calculated discharge, while the values given for 15°C and atmospheric pressure are used as constants for the heat capacity (c_p) and the density (ρ_W) of the water without any relevant loss of accuracy.
In the net shortwave radiation (R_K) a shade factor is considered along with the global radiation and the albedo of the body of water. This shade factor combines the shade cast on the river by shore vegetation and horizon heightening.
To determine the net long-wave radiation (R_L) the thermal radiation of the river is simulated with the Stefan-Boltzmann law. The long-wave atmospheric reabsorbed radiation is calculated under consideration of the air temperature, humidity and the degree of cloudiness.
The evaporation or condensation at the river surface and the resulting latent heat flux (H_L) can be calculated with different aerodynamic models (Dalton approaches) under

consideration of the water temperature, the current vapour pressure in the air and the wind velocity. In the WBTM used here, the approach by Rinsha and Domschenko (cit. in LAWA 1991) is used. The fact that the measured values of the climate stations are often not representative of the wind velocities in the river is allowed for by means of a wind-break factor.
In the simulation of the sensible heat flux (H_F) it is assumed that the turbulent exchange term for heat is equal to that for water. The turbulent mass flux of sensible heat is thus calculated under consideration of the Bowen relationship, analogous to the evaporation.
The temperature of the riverbed and the resulting heat exchange with the body of water are illustrated in a simplified manner with the help of a single-layer sediment model.
As well as the heat exchange processes in the flowing section, local heat sources such as the heat discharge from thermal power plants or wastewater treatment plant processes with a defined water temperature can also be considered. Below the point of discharge the calculations continue with the arithmetic mixed temperature.
Therefore, with the physically-based approach the space and time distribution of the water temperature can be shown for the flowing section of the entire model area.

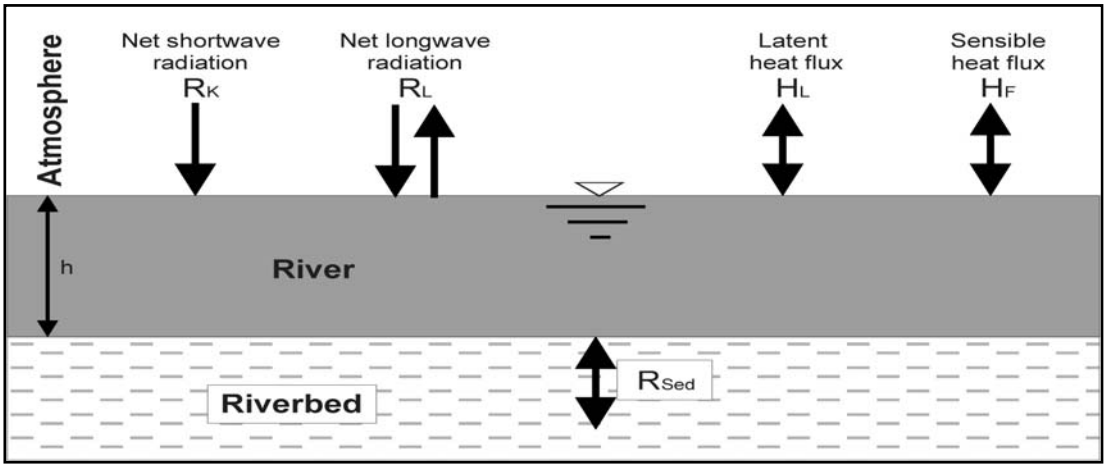

Figure 2: Heat exchange processes allowed for in the WBTM on the flowing section

Local regression model for the water temperature

The physically-based simulation of the water temperature described above generally produces good agreement with measured values. However, even better results may be achieved selectively in shallow running waters with spatially and time-related variable shade, which are not influenced by heat discharges. Therefore, regression models can also be given in the WBTM for individual points of the river network in order to calculate the water temperature. The results of the regression model that are valid for the defined points in the river system can be used as a marginal condition for the physically-based calculation in the river section that lies beneath.
Regression models are of particular importance in this case, as with their help those water temperature marginal conditions that are not covered by a WBTM can also be given.
The general form of the multiple, non-linear regression model was derived on the basis of fundamental findings regarding the connection between air and water temperature (Mohseni& Stefan 1999) as well as further theoretical considerations on the influence of the discharge and the riverbed. Taking account of these fundamentals, it was possible to show that water temperature can best be predicted with the exclusive use of air temperature and perhaps discharge as predictors (LfU 2005).

The parameter values of the regression model for one point in the river network can be determined based on measured air temperature and series of water temperature measurements as well as any series of discharge measurements.

Appendix C. Description of the model SOBEK (1D / 2D modelling suite)

1. General

Worldwide, there is a growing need for integral water solutions. We need protection from excess water in order to live safely in deltas and river basins, and our water systems also need to be clean and sustainable. To support water authorities, consultancy firms, research institutes and universities, Deltares offers an integrated modelling suite called SOBEK for the integral simulation.

SOBEK is a powerful modelling suite for flood forecasting, optimisation of drainage systems, control of irrigation systems, sewer overflow design, river morphology, salt intrusion and surface water quality. The components within the SOBEK modelling suite simulate the complex flows and water-related processes in almost any system. The components represent phenomena and physical processes in an accurate way in one-dimensional (1D) network systems and on two-dimensional (2D) horizontal grids.

It has been developed – and is being further developed – jointly with Dutch public institutes and governmental organisations, research institutes, universities and private consultants all over the world.

2. Integrated approach

SOBEK offers one software environment for the simulation of all management problems in the areas of river and estuarine systems, drainage and irrigation systems and wastewater and storm water systems. This allows for combinations of flow in closed conduits, open channels, rivers overland flows as well as a variety of hydraulic, hydrological and environmental processes.

Picture 1: Example integrated model (FLOW 1D Pipe and FLOW 1D Open water plus several RR models), Hong Kong.

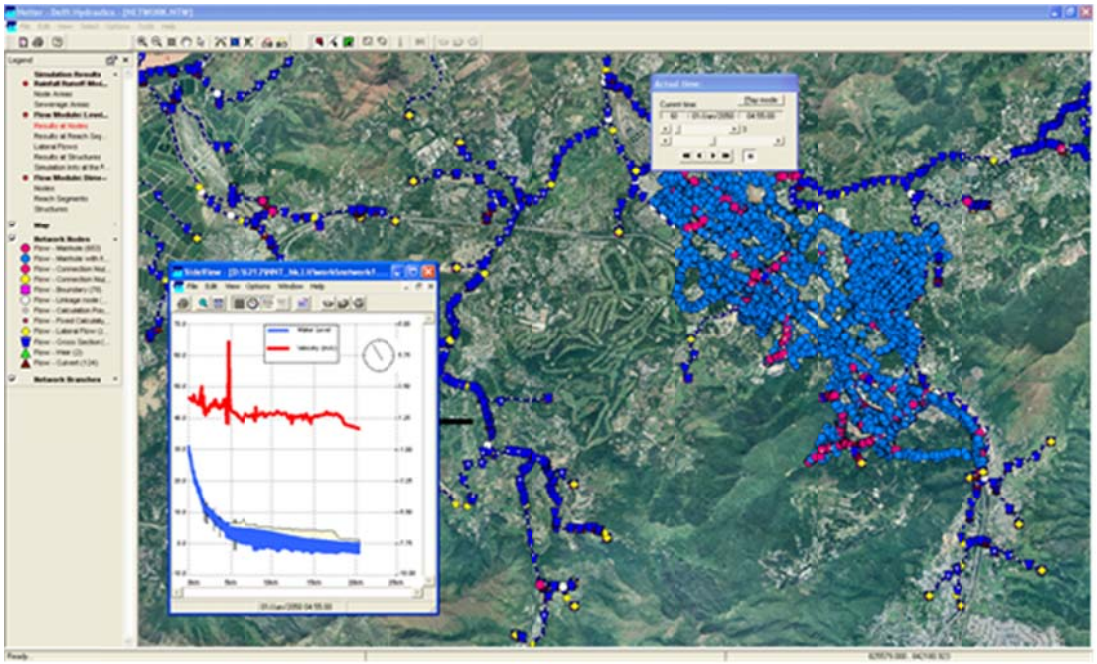

2.1. A powerful hydrodynamic 1D/2D simulation engine

The hydrodynamic 1D/2D simulation engine is the computational core of the SOBEK. This engine is used in all FLOW components within the SOBEK modelling suite. Thus allowing the combined simulation of pipe, river-, channel- and overland flow through an implicit coupling of 1D and 2D flow equations, SOBEK is the ideal tool for studying the effects of dam breaks, river floods, dike breaches, urban flooding etc.

2.2 Robustness of numerical operations

The hydrodynamic 1D/2D simulation engine is equipped with a very robust scheme for numerical computation. It also guarantees mass conservation, even in the case of transitions through suddenly varying cross-section shapes. The engine combines computations of sub-critical and supercritical flow, at scales selected by the user. It handles the flooding and drying of channels without the use of artificial methods such as the Preissmann slot.

2.3 Numerical efficiency

The hydrodynamic 1D/2D simulation engine has a very efficient numerical solution algorithm; this is based upon the optimum combination of a minimum connection search direct solver and the conjugate gradient method. It also applies a variable time step selector, which suppresses the waste of computational time wherever this is feasible.

2.4 Size of models

The size of the model is limited only by the size of the internal memory of the computer used.

3. Components

SOBEK allows you to simulate the interaction of water and water-related processes in time and space. The package is mostly used for the modelling of integrated water systems for water management, design, planning and policy making. SOBEK consists of a number of well-tested and validated components, which are linked to and integrated with oneanother. These components are:

3.1 FLOW 1D Open water

This component works with the complete de Saint Venant Equations, including transient flow phenomena and backwater profiles. It models any cross-section (open and closed), including asymmetrical profiles and y-z profiles. It even allows you to define different sub-sections within a cross-section, using alternative resistance formulations and/or coefficients in each sub-section. The hydrodynamic 1D/2D simulation engine has an automatic drying and flooding procedure that is 100% mass conservative. The engine can deal with steep canals with supercritical flow, and moving hydraulic jumps are simulated as easily as canals with a mild slope and sub-critical flow. Complex networks of any size with internal loops and branches are easily handled without any problems. You can specify nearly any type of hydraulic structure (pumps, weirs, gates, culverts, sluices and bridges of virtually any shape and dimension). It may also take into account deposited soil layers partially blocking culverts and bridges. Various options for the automatic control of the structures are available as standard, including time control, hydraulic control and PID control with both fixed and variable set-points. Sediment transport capacity can be computed and visualised on the network. The effects of wind on water levels can be modelled, by specifying the wind force and direction as constants or time series. All possible boundary conditions and initial conditions can be applied. Lateral in- and outflows can be specified as constants, time-based, formula-based or read automatically from the RR Open water component (Rainfall Runoff). Lateral flows from other Rainfall Runoff components can easily be coupled. The FLOW 1D Open water component interfaces completely with all SOBEK components to provide an integrated model of the water system.

3.2 FLOW 1D Pipe

This component uses the complete de Saint Venant Equations, thus including backwater and transient flow phenomena. It models a wide variety of cross-sections and manhole shapes (including user-defined ones) and allows you to build up your own cross-section and manhole database. It is specially designed to handle large and complex sewer networks on an ordinary PC, where the computation time is only linear with the size of the network and independent of its complexity. The hydrodynamic 1D/2D simulation engine has an automatic drying and pressurised procedure and handles real supercritical flow and is always 100% mass conservative. It uses a self-selecting time step so your computer won't crash and accuracy is guaranteed. All possible boundary conditions can be specified by you or are automatically applied. The FLOW 1D Pipe component includes rainfall runoff inflow, dry weather flows and processes for various types of paved areas, such as streets, roofs and parking lots. You may define your own time and spatially varied rainfall pattern, or historical data of storm events and long-time series with or without dry periods. Sediment transport computation shows where sediment might be deposited; interfaces completely with the FLOW 1D Open water component to provide an integrated model of the urban water system and its environment.

3.3 FLOW 2D Overland

This component is fully integrated with the FLOW 1D Open water and FLOW 1D Pipe components for accurate flood simulation of river systems, polder areas, dikes / levees / dam breaches, streets, etc. It is based upon the complete de Saint Venant Equations. The hydrodynamic 1D/2D simulation engine simulates steep fronts, wetting and drying processes, sub critical and supercritical flow. And it handles multi-domains and nested multi-domains. The FLOW 2D Overland component includes rainfall on the 2D grid.

Picture 2: Example flood modelling Daly River, Australia.

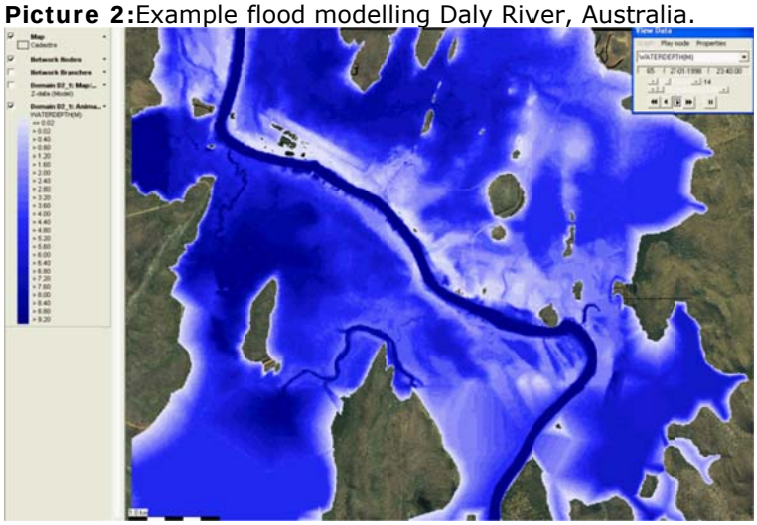

3.4 RR Open water

This component contains a library of Rainfall Runoff models from polder sub-catchment scale up to river catchment scale, such as HBV and SCS. The catchment areas can easily be modelled in a lumped or detailed manner with no restriction on the number of catchment areas. The catchment areas can be modelled in any detail using land elevation curves, soil characteristics, land cultivation, drainage characteristics etc. It distinguishes between various rainfall run-off processes such as surface run-off, sub-soil drainage and storage in saturated and unsaturated areas, taking crop evaporation and capillary rise into account. The RR Open water component uses separate storm events or long time series of meteorological data for statistical analysis. You can input your own rainfall patterns or use historical data, and model any number of rainfall gauges taking the spatial variation into account. It can model both flood events and dry spells. This component can be used in combination with the FLOW 1D Open water component and the RTC component.

3.5 WAQ 1D

This component is based on the water quality 1D/2D/3D simulation engine which offers you more than 30 years of collective water quality modelling experience worldwide. It models almost any water quality variable and its related water quality processes. This component is highly flexible due to the many standard options and user-defined options available (Postma et al. 2003). It uses a library of processes and substances, including water temperature, eutrophication, nutrients, bacteria, oxygen, phytoplankton, heavy metals etc. The interactive processes editor allows you to select the water quality variables and processes you want to model. To analyse the origin of mass in any water system, fraction computations can be easily done and trace e.g. pollutants from its source throughout the network. The state-of-the-art numerical schemes of the water quality 1D/2D/3D simulation engine use a finite volume approach and the component display mass balances. It is fully integrated with the standard user interface.

When water temperature is modelled to predict the effects of heat discharges, an excess temperature model is often used. In an excess, or surplus, temperature model the water temperature resulting from heat discharges is modelled on top of a usually forced ambient background temperature. When water temperature is modelled to study e.g. changes in climate, a more elaborated heat balance model approach is usually followed. In a heat balance model the ambient water temperature is calculated from the heat fluxes across the water air surface. Meteorology is the main forcing for heat balance models.

WAQ supports these two major approaches and allows for a combination of the two as well.

Specific postprocessing tools related to water temperature modelling are implemented, e.g. calculating the heat load capacity, which is the amount of heat that may be discharged before an ambient water temperature standard, e.g. 25ºC, is exceeded.

Picture 3: Example of temperature in waste water and sewer pipe and surrounding soil (to study the potential to harvest thermal energy from waste water).

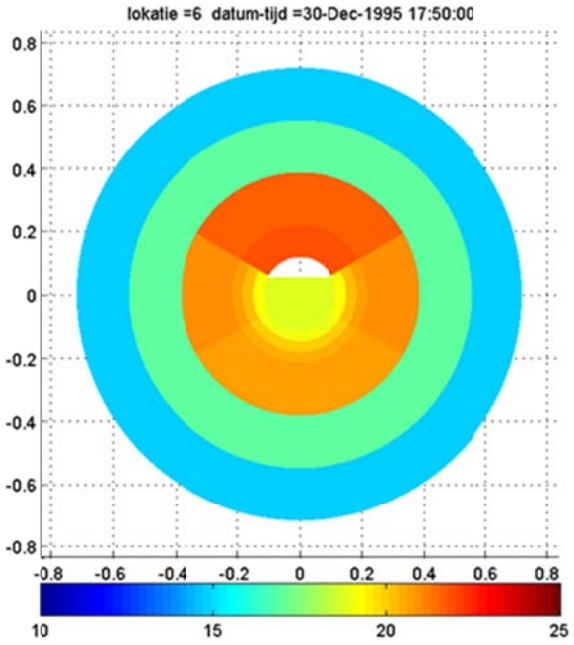

Picture 4: Example longitudinal plot (Maxau-Lobith) for showing the simulated discharge (top) and below simultaneously the water temperature and excess water temperature (blue) and the excess water temperature (red) caused by thermal discharges.

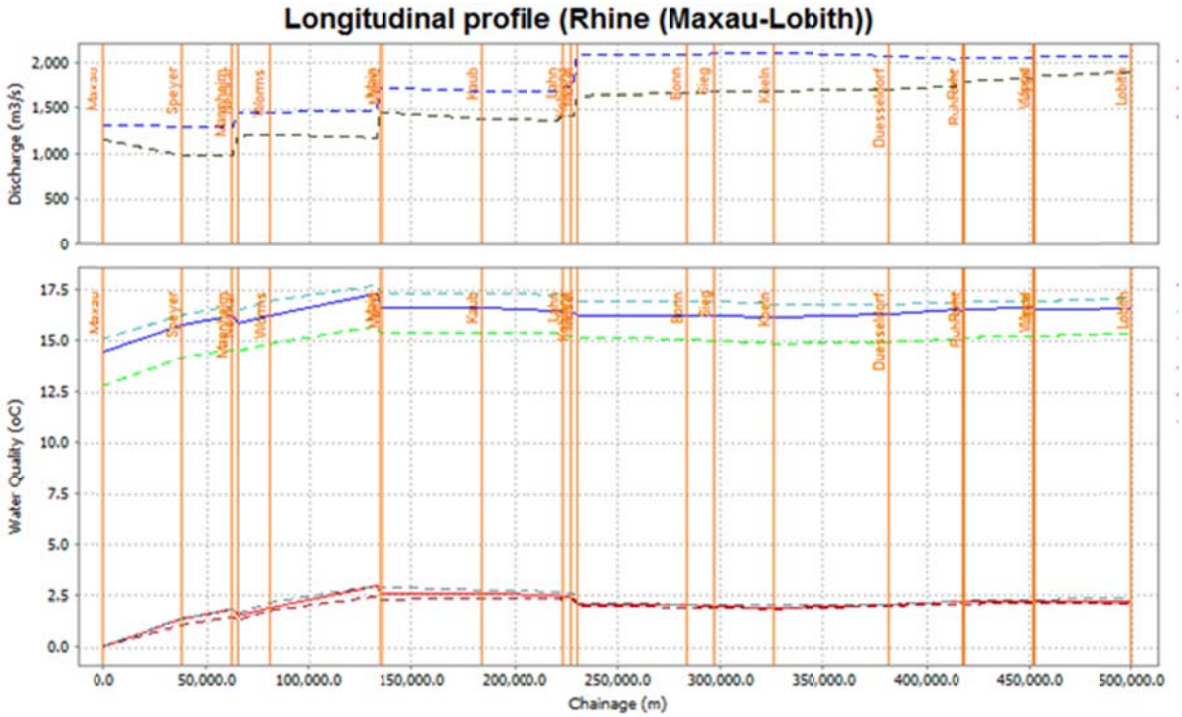

3.6 RTC

Real-time control often saves money in the construction, alteration and management of the water system infrastructure. The RTC component shows to what extent the existing infrastructure can be used in a better way. It allows you to simulate complex real-time control of all hydraulic structures in rivers, canals, irrigation and drainage systems and/or pipe networks. This component allows the system to react optimally to actual water levels, discharges, (forecasted) rainfall, by controlling gates, weirs, sluices and pumps. The RTC component can also be linked to Matlab, the industrial standard for control engineers, and even allows you to define your complete control system in Matlab. It enables you to intervene in events taking place within your water system. This component helps you make informed choices about automation and the best water control strategy. All standard irrigation automation concepts can be handled with this component.

3.7 Graphical User Interface

The Graphical User Interface (GUI) is one of the most user-friendly in the market. Under the umbrella of this GUI, the components, which can be purchased separately, combine into an exceptionally versatile and easy-to-use power package. The GUI allows the user to visualize model input, reference data and simulation results as time series and animations of one and two dimensional data sets on the map and in side views. The SOBEK modelling suite is open for additional pre and post processing tools, such as the QUICKIN tool, a powerful editor of grid related data, such as bathymetries for the FLOW 2D Overland component, running standalone and as ArcGIS plug-in.

Picture 5: QUICKIN, a powerful editor of grid related data, such as bathymetries.

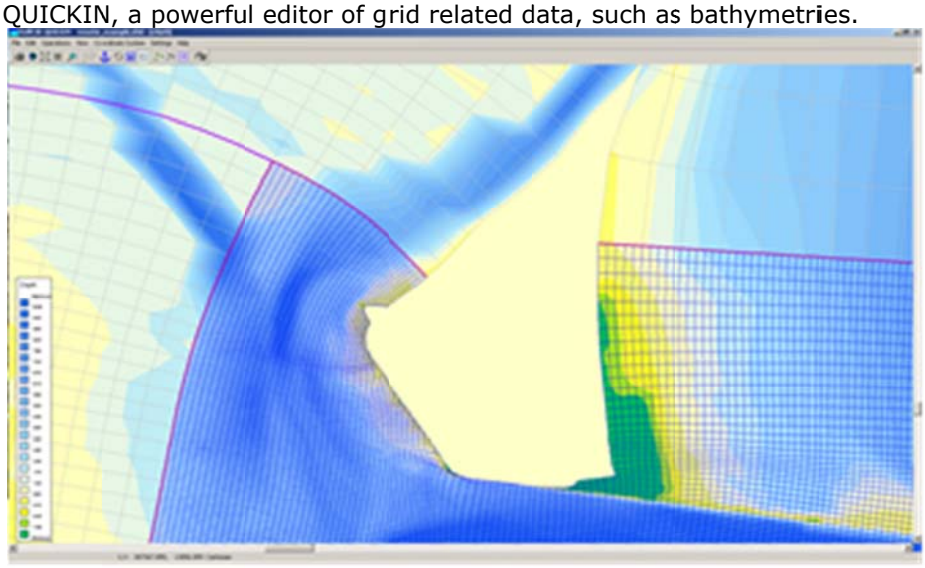

The SOBEK components are also available as plug-ins in the open operational framework called Delft-FEWS. Within Delft-FEWS the components can either be deployed in a stand-alone, manually driven environment, or in a fully automated distributed client-server environment.

Picture 6: Example Graphical User Interface of Delft-FEWS with SOBEK components as plug-ins, Rhine Delta.

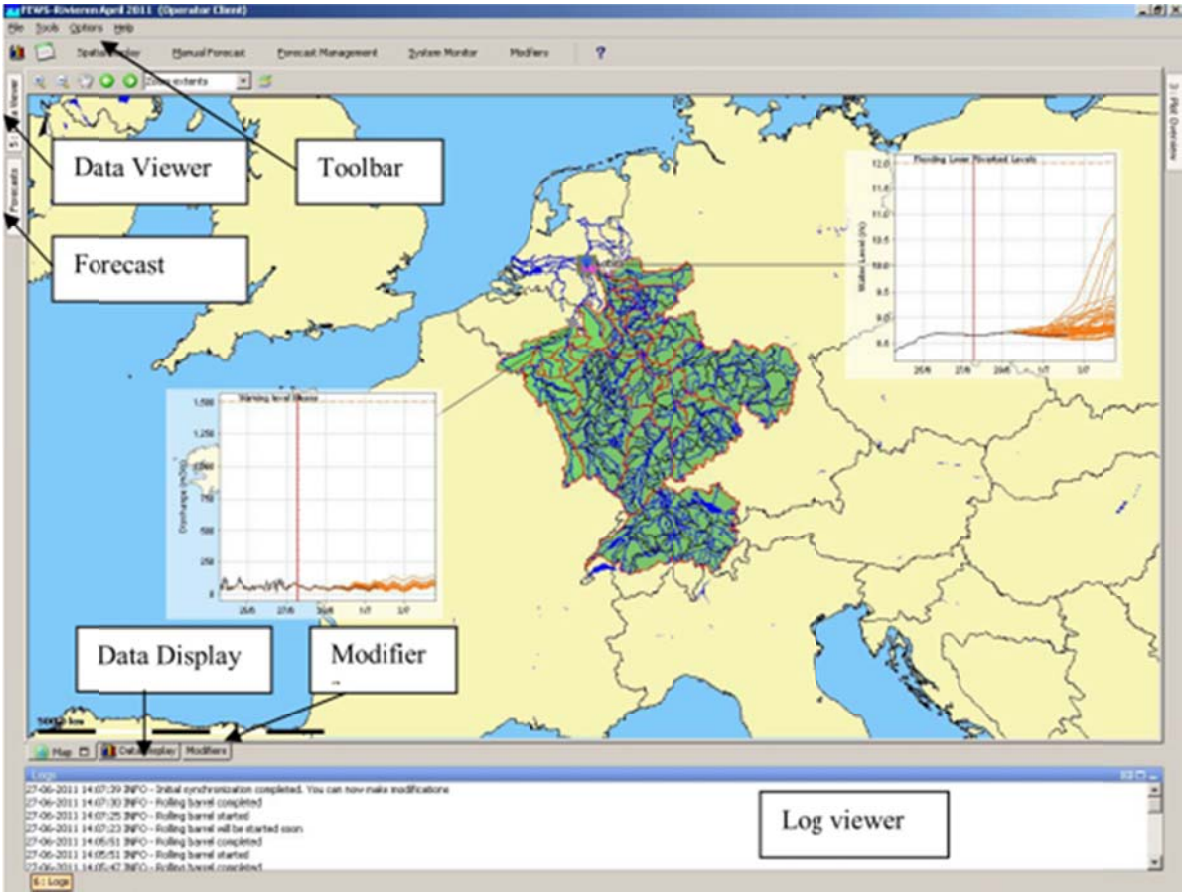

4. Miscellaneous

Validation

The validation of a modelling system such as SOBEK requires continuous attention. Even though the individual components of the system have been thoroughly tested during their development, the system as a whole requires intensive testing and validation too.

System requirements

SOBEK is supported on Microsoft Windows. For details, please visit our website. The advised minimum requirements are a configuration consisting of:

Tabel.1: System requirements

	Minimal	Preferred
Processor	1 GHz	3 GHz
Memory	64 Mb	128 Mb
Disk free	100 Mb	1 Gb

Services

The SOBEK service desk is the user's instantly accessible contact point for all questions and problems concerning the software. The support manager answers the majority of questions instantly or takes responsibility that a timely reply is given by one of the other SOBEK team members.New versions of SOBEK will be released once a year to all users, providing their package is covered by a valid maintenance agreement.

Deltares organizes once a year an international SOBEK user conference. Multiple smaller SOBEK user meetings are organized at international conferences world-wide; providing excellent venues to get updates on latest developments and to meet other SOBEK users. Please visit the www.deltaresacademy.com for all info about our SOBEK training courses.

Ongoing Developments

Developments of the SOBEK system currently include MOR 1D (morphology) component (1D-3D), WAQ 2D (water quality), OpenMI and OpenDA, Flexible mesh support (an integrated engine based on 1D networks and 3D/2D layered mesh of mixed triangles, quadrilaterals, and more complex cells) and DeltaShell, open flexible modelling suite for 0D-3D models.For our beta testing program, please contact sobek.sales@deltares.nl.

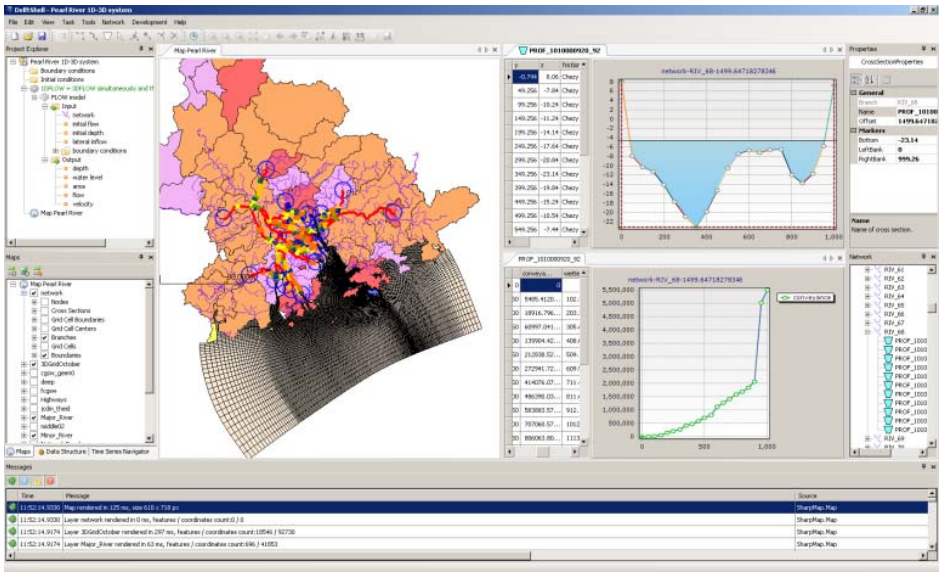

Picture 7: Impression of the new user interface: DeltaShell, open flexible modelling suite for 0D-3D models.

Appendix D. Description of the model QSim

1. The water quality model QSim

The water quality model QSim(**Q**uality **Sim**ulation) of the Federal Institute of Hydrology (BundesanstaltfürGewässerkunde, BfG) describes in a mathematical way the complex chemical and biological processes in running waters. An important feature is the close linkage of hydraulic with ecological modules. The most important biological processes of the oxygen and nutrient balance as well as the development of phytoplankton and zooplankton and the processes at the river bottom (Fig. 1, Table 1) are calculated in the model. QSimis suited to simulate processes in simple channels as well as in complex river networks and water bodies with variable flow directions. Furthermore, engineered river stretches with groynes and their influence on materials content and temperature layers, with their resulting vertical materials grades,can be modelled with a quasi-2D approach. One of the main results is the simulation of annual cycles of the oxygen content and other water quality parameters, as well as biological variables, such as algal biomass, along a river continuum.

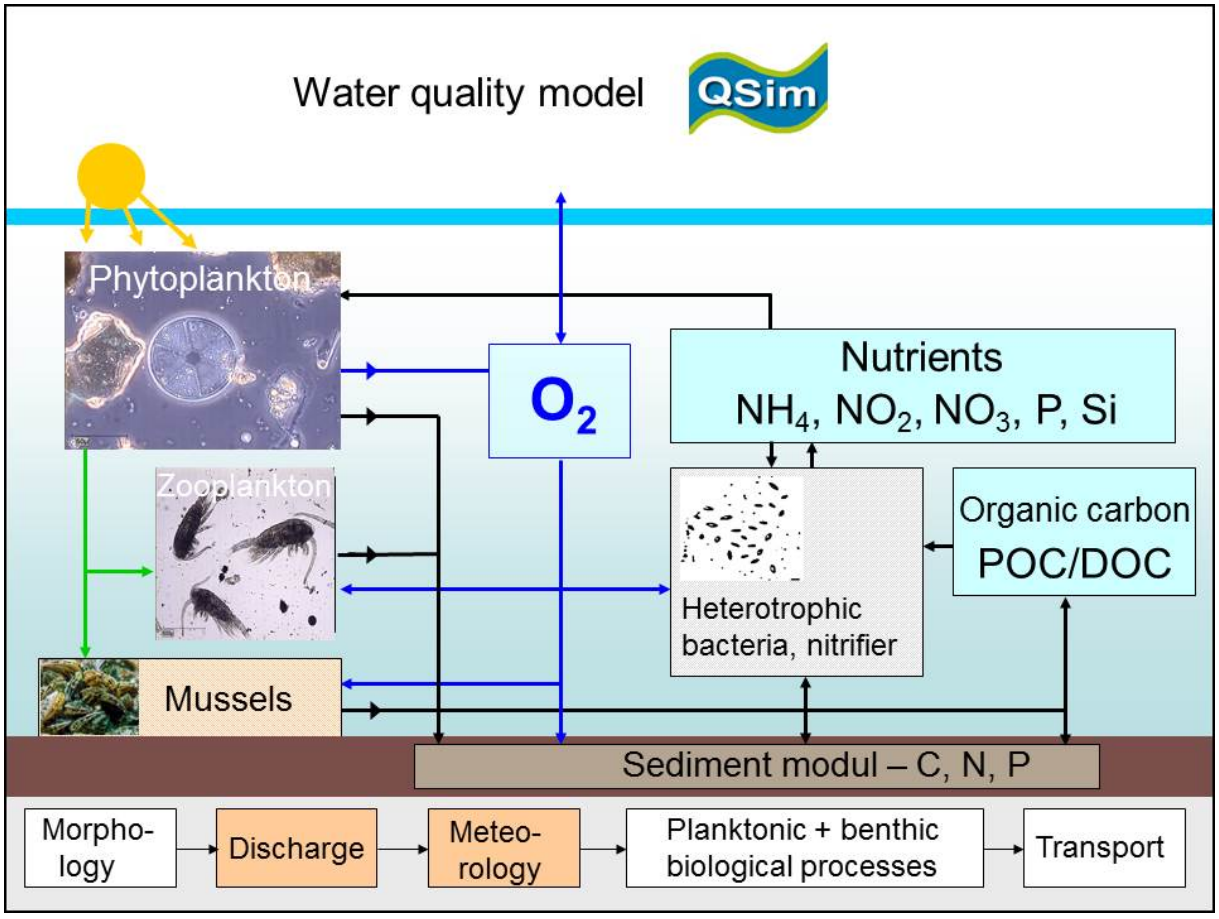

Fig. 1: Model structure and functionality of QSim

QSimis used in the BfGprimarily to determine and assess the impact of engineering measures on the water quality of federal waterways. In addition, questions arising from the water industry and catchment management as well as climate change issues are addressed with QSim. The current version,QSim 13.0, is the result of 30 years of continuous development work and experience from a wide variety of applications for different

river systems.QSimthus integrates model development, specialist application and basic hydro-ecological research at the BfG.The QSim heat balance module is described below.

Table 1: Processes and input variables of QSim

Processes	Input variables
Simulation of discharge Sedimentation Heat balance Underwater light climate Calcium-carbonate balance Oxygen and nutrient balance Bacterial growth Nitrification Algal growth Macrophyte growth Zooplankton growth Growth of benthic filter feeders	**Morphological / hydrological**: flux geometry, discharge
	Meteorological: global radiation, air temperature, cloud type and cover, humidity, wind velocity
	Physical / chemical: water temperature, oxygen, chemical oxygen demand, ammonium, nitrite, nitrate, o-phosphates, total N and P, silicate, pH, alkalinity, seston, Ca, conductivity
	Biological: Biochemical oxygen demand (C- and N-derived), flagellates, biomass of planktonic algae (chlorophyll a) and proportion of diatoms, green algae and cyanobacteria, zooplankton (rotifier density), nitrifyingbacteria(*Nitrosomonas*and*Nitrobacter*), benthic algae, macrophytes, benthic filter feeders (*Dreissenapolymorpha*,*Chelicorophiumcurvispinum*)

2. The water balance module

2.1 Components of the water balance

The basis of all common methods for calculation the heatingof a body of running water is the simplified heat balance equation. On its basis the heat balance of the river is created, with which the temperature changes of the river can be quantified per time unit.
The components considered in the simplified heat balance equation are essentially the influences from radiation (q_S), evaporation (q_V), convection (q_K), the riverbed (q_U,q_{US}) and direct discharges (q_E) on the river. All other possibly influencing components, such as heat discharge from shipping or chemical or biological processes, are usually only of secondary importance from a quantitative perspective. Therefore, these influences, together with influences from the influx of groundwater – which may in some circumstances be greater, but usually more difficult to quantify –, are considered in the calibration.
Thus the simplified heat balance equation is as follows:

$$\frac{\partial TW}{\partial t} = \frac{q_S - q_V - q_K + q_{US} - q_U + q_E}{c_W * H * \rho_W} \qquad (1)$$

with:

q	Overall heat flux density in kJ/(h m^2)
T_W	Watertemperature
t	Time (time unit)
q_S	Heat flux density from radiation in kJ/(h m^2)
q_V	Heat flux density from evaporation in kJ/(h m^2)
q_K	Heat flux density from convection in kJ/(h m^2)
q_E	Heat flux density from direct discharge in kJ/(h m^2)
c_W	Special heat capacity of water = 4.1868 10^3 J/(kg K)
h_m	Average water depth in m
ρ_W	Density of the water = 1,000 kg/m^3

Because the time interval of one hour (h) is used in the quality simulation, the specification of the (empirical) formula constants is given with reference to the unit kJ/(h m^2). Thus the conversion factor for the common specification in W is: 3.6 kJ/h = 1J/s =1 W
However, this equation of the heat balance cannot be solved explicitly, as the different components to be considered often do not depend linearly on the temperature and the local reference system also often changes with the flowing wave. Therefore there are many different calculation methods to solve the heat balance equation, which can differ greatly both in their formula approachesand in the manner of their approximate solution. The approaches used in QSim to calculate the individual components are described below.

2.2 Individual components of the heat balance

2.2.1 Radiation components

The influence of radiation on the water balance of a river is divided into the influence from global radiation, atmospheric radiation and the radiation of the water surface, i.e.:

$$q_S = q_{S,G} + q_{S,A} - q_{S,W} \qquad (2)$$

with:

q_S	Heat flux density from radiation in kJ/(h m^2)
$q_{S,G}$	Heat flux density from global radiation in kJ/(h m^2)
$q_{S,A}$	Heat flux density from atmospheric radiation in kJ/(h m^2)
$q_{S,W}$	Heat flux density from the radiation of the water surface in kJ/(h m^2)

Although it is certainly possible to determine the overall radiation balance by measurements, the measuring methods used often deliver insufficiently precise results, so that it is generally unavoidable to obtain some of the values sought by means of empirical observation or the calculation of the individual components.

Global radiation
Global radiation, $q_{S,G}$, is the sum of direct sun radiation and diffuse sky radiation. However, only part of this radiation is actually converted into heat. The rest, in general ca. 15 %, is reflected on the water surface. Global radiation always has a positive value. It depends on

- Position of the sun
- Degree of cloudiness
- Steam content of the air
- Distribution of temperature
- Horizon shielding.

Due to the diverse and difficult to quantify dependencies, measured global radiation values are used in QSimfor further calculations. This proportion of the heat radiation always has positive values.

Atmospheric radiation
Atmospheric radiation $q_{S,A}$ is the radiation that results from the reflection on steam or carbon dioxide particles at great altitudes. It is therefore dependent essentially on the following variables:

Steam content of the air

Position of the sun

Distribution of temperature

This proportion of the overall heat balance also always has positive values.
As there are generally no altitude-differentiated measurements of the steam content and temperature of the environment, the atmospheric radiation is determined in QSimwith the help of empirical observations, of which, according to a study by KASTEN (1989) the formula by SWINBANKprovides the best results for a cloudless sky:

$$q_{S,A,0} = 9{,}3 \cdot 10^{-6} \cdot \sigma \cdot \left(T_{L,tr} + 273{,}16\right)^6 \qquad (3)$$

with:

$q_{S,A,0}$	Atmospheric radiation in a cloudless sky
σ	Stefan-Boltzmann constant (σ = 2.0411 10^{-7} kJ/(h m^2 K^4) = 5.6698 10^{-8} W/(m^2 K^4))
$T_{L,tr}$	Air temperature, measured on a dry thermometer in °C

In a cloudy sky, atmospheric radiation increases due to the reflection on water drops and ice crystals on the underside of the clouds. This increase is dependent on the cloud cover and the height of the underside of the clouds above the earth's surface.

If the height of the underside of the clouds is placed in relation to the cloud type, the influence of the cloudiness can be considered by means of a coefficient $k_{B,A}$. This is calculated, depending on cloud type (see Table 2) and cloud coverage $\alpha_B$at:

$$k_{B,A} = 1{,}0 + f_{Typ}\left(\frac{\alpha_B}{8}\right)^{2{,}6} \qquad (4)$$

with:

$k_{B,A}$	Coefficient to allow for the cloudiness
α_B	Degree of cloud coverage in eighths of the sky between 0 and 8 according to DWD
f_{Typ}	The factor $f_{Typ}$is determined correspondingly, depending on cloud type. For the modelling of the Rhine, Cirrostratus is taken throughout as the cloud type.

Table 2: Factor for calculating the influence of cloudiness on atmospheric radiation, see Equation(4)

No.	Cloud type	f_{Typ}	No.	Cloud type	f_{Typ}
1	Cirrus	0.04	6	Nimbostratus	0.22
2	Cirrocumulus	0.06	7	Stratocumulus	0.23
3	Cirrostratus	0.08	8	Stratus	0.24
4	Altocumulus	0.17	9	Cumulus	0.20
5	Altostratus	0.20	10	Cumulonimbus	0.25

With $k_{B,A}$ =1 in a cloudless sky, i.e. a_B =0 in Equation(4), the cloud-dependent heat radiation of the atmosphere is then calculated by the cloudiness factor to:

$$q_{S,A} = k_{B,A} \cdot q_{S,A,0} \quad (5)$$

Radiation from the water surface

Although a river absorbs most of the radiation that occurs, a certain amount of radiation is emitted back from the body of water. This (back-) radiation from the water surface is proportional to the fourth power of the temperature of the body of water and enters the overall radiation balance with a negative sign.

The heat radiation of the water is determined by means of the Stefan-Boltzmann law for a grey bodyand depends on the absolute temperature of the water surface and the effective long-wave emissivity $_W$ ab.

The equation used in QSim to calculate the heat radiated from the water surface is:

$$q_{S,W} = \varepsilon_w \cdot \sigma \cdot (T_W + 273{,}16)^4 \quad (6)$$

with:

$_W$ Effective long-wave emissivity = 0.97

σ Stefan-Boltzmann constant (σ = 2.0411 10^{-7} kJ/(h m^2 K^4) = 5.6698 10^{-8} W/(m^2 K^4))

T_W Watertemperature

2.2.2 Evaporation and condensation

In contrast to the radiation components in the heat balance, which lead to an increase in the river temperature, evaporation generally contributes not insignificantly to the cooling of the body of water. Evaporation arises from the pressure balance of the vapour pressure between the water surface and the layer of air above. If the vapour pressure at the water surface is greater than that of the air, water evaporates from the river. As more or less evaporation heat is required for this process, depending on the water temperature, the body of water cools down. In the inverse case, water condensates from the air into the river, which represents an influx of heat, but this is generally not the case. Depending on the vapour pressure conditions, the evaporation term in the heat balance can therefore take on both positive and negative values. In order to quantify the term, the saturated vapour pressure at the water-air phase interface and – not insignificantly – the wind velocity are important. Here, too, empirical observations are used to evaluate the components. The empirical constants used for this purpose are location- and river-dependent and must be calibrated. Thus, even the selection of the correct formula is essential to the quality of the results.

a) In QSim, the evaporation rate $h_V$is calculated on the basis of the approach by DALTON. Its general formula is:

$$h_V = (a + b \cdot v_{Wind}^C) \cdot (p_S - p_D) \frac{1}{24.000} \frac{p_{L,Ort}}{p_{L,Meer}} \quad (7)$$

with:

p_S	Saturated vapour pressure in the water temperature of the water surface in hPa
p_D	Partial vapour pressure in the air temperature, measured on a dry thermometer in hPa
v_{Wind}	Wind velocity in m/s
$p_{L,Ort}$	Air pressure at local altitude in hPa
$p_{L,Meer}$	Air pressure related to sea level in hPa

Here, coefficient a describes the wind-independent part of the evaporation, while coefficients b and c describe the wind-determined proportion to be overlaid. The factor 1/24.000 is produced from the conversion of the evaporation rate $h_V$from mm/d to m/h.

Of the various different approaches for the empirical constants a, b and c, the approach of the WORLD METEOROLOGICAL ORGANISATION (WMO) from 1966 is used in QSim, in which the constants adopt the following values:

a=0.130 b = 0.0936 und c=1

The saturation vapour pressure at the water surface is calculated from the water temperature $T_W$at

$$p_S = 6{,}10780 \cdot e^{\frac{17{,}08085 \cdot T_W}{234{,}175 + T_W}} \quad (8)$$

The partial vapour pressure of the air with the air temperature measured on a dry thermometer is calculated from:

$$p_D = \frac{6{,}1078 * e^{\frac{17{,}08085 + T_{L,tr}}{234{,}175 + T_{L,tr}}}}{100} * F_{rel}$$

Then, from the evaporation rate $h_V$we get the evaporation heat (heat flux density) $q_V$by means of the following interrelation:

$$q_V = \rho_W \cdot c_V \cdot h_V \quad (9)$$

with:

ρ_W	Density of the water in kg/m³
c_V	Latent evaporation heat in kJ/kg
h_V	Evaporation rate according to Equation (7) in m/h

Finally, the latent evaporate heat $c_V$is calculated in dependence on the water temperature T_W at:

$$c_V = 2501{,}7 - 2{,}366 \cdot T_W \quad (10)$$

If the vapour pressure at the water surface is lower than that of the layer of air above it, water condensates instead of evaporating. In this (somewhat rare) case, a corresponding heat gain occurs. Depending on the vapour pressure conditions (p_S-p_D), the evaporation term can therefore take on negative or positive values.

2.2.3 Convection

Convection is the direct heat exchange between the air and the surface of the water. It takes place only when the temperature of the air and the water differ and is, like evaporation, dependent on wind velocity. The influence of convection on the heat balance of a river is usually much lower than that of evaporation.

Of the various possible approaches, the approach according to LAWA (1991) is used in QSim, for which the convective heat flux is calculated according to the following formula:

$$q_K = q_V \cdot \frac{T_W - T_{L,Tr}}{1{,}53 \cdot (p_S - p_D)} \qquad (11)$$

with:

q_V	Heat flux density from evaporation according to Equation (9) in kJ/(h m^2)
T_W	Watertemperature in °C
$T_{L,Tr}$	Air temperature, measured on a dry thermometer in °C
p_S	Saturation vapour pressure in the water temperature at the water surface in hPa
p_D	Partial vapour pressure in the air temperature, measured on a dry thermometer in hPa

Depending on the temperature conditions between air and water, the convection term can take on positive or negative values.

2.2.4 Direct heat discharge

In addition to the aforementioned more or less natural components of the heat balance, direct heat-related discharge in the form of cooling water forms the most important term in this balance to asses cooling water discharge into a river. However, this term includes not only the heat discharge due to cooling water discharge but also heating due to the influx of usually warmer tributaries, or cooling due to groundwater influx.

$$q_E = c_W \cdot \rho_W \cdot v_E \cdot \Delta T \qquad (12)$$

with:

q_E	Heat flux density from direct discharge in kJ/(h m^2)
c_W	Special heat capacity of water = 4.1868 10^3 J/(kg K)
ρ_W	Density of the water = 1,000 kg/ m^3
v_E	Discharge speed = Q_E/A_E (point source) resp. q_E/L_E (line source) in m/s
ΔT	Temperature rise range, temperature difference (T_1-T_2) in K

To simplify calculation, we assume a homothermal (consistently warm) body of water and the immediate and complete mix of the fluxes for a point-source discharge, although more or less distinct – depending on the type of flow process – zones and layers of different temperatures are formed beneath the point of discharge. However, this simplification is permissible for most formulations (e.g. large-scale heat balances).

2.2.5 Water temperature

The water temperature, respectively the change in water temperature due to heat exchange at the water surface is calculated from the heat balance equation:

$$\frac{\partial T_W}{\partial t} = \frac{q(T_W, t)}{c_W \cdot h \cdot \rho_W} \tag{13}$$

respectively for atimestepΔt:

$$\Delta T = \frac{q(T_w, t)}{C_w * h * \rho_w} * \Delta t$$